Building Applied and Back Insulated Photovoltaic Modules:

Thermal Models

by

Jaewon Oh

A Thesis Presented in Partial Fulfillment
of the Requirements for the Degree
Master of Science in Technology

Approved November 2010 by the
Graduate Supervisory Committee:

Govindasamy Tamizhmani, Chair
Bradley R. Rogers
Narciso F. Macia

ARIZONA STATE UNIVERSITY

December 2010

ABSTRACT

Building applied photovoltaics (BAPV) is a major application sector for photovoltaics (PV). Due to the negative temperature coefficient of power output, the performance of a PV module decreases as the temperature of the module increases. In hot climatic conditions, such as the summer in Arizona, the operating temperature of a BAPV module can reach as high as 90℃. Considering a typical 0.5%/℃ power drop for crystalline silicon (c-Si) modules, a performance decrease of approximately 30% would be expected during peak summer temperatures due to the difference between rated temperature (25℃) and operating temperature (~90℃) of the modules. Also, in a worst-case scenario, such as partial shading of the PV cells of air gap-free BAPV modules, some of the components could attain temperatures that would be high enough to compromise the safety and functionality requirements of the module and its components. Based on the temperature and weather data collected over a year in Arizona, a mathematical thermal model has been developed and presented in this paper to predict module temperature for five different air gaps (0”, 1”, 2”, 3”, and 4”). For comparison, modules with a thermally-insulated (R30) back were evaluated to determine the worst-case scenario. This thesis also provides key technical details related to the specially-built, simulated rooftop structure; the mounting configuration of the PV modules on the rooftop structure; the LabVIEW program that was developed for data acquisition and the MATLAB program for developing the thermal models. In order to address the safety issue, temperature test results (obtained in accordance with IEC 61730-2 and UL 1703 safety

standards) are presented and analyzed for nine different components of a PV module, i.e., the front glass, substrate/backsheet (polymer), PV cell, j-box ambient, j-box surface, positive terminal, backsheet inside j-box, field wiring, and diode. The temperature test results obtained for about 140 crystalline silicon modules from a large number of manufacturers who tested modules between 2006 and 2009 at ASU/TÜ V-PTL were analyzed and presented in this paper under three test conditions, i.e., short-circuit, open-circuit, and short-circuit and shaded. Also, the nominal operating cell temperatures (NOCTs) of the BAPV modules and insulated-back PV modules are presented in this paper for use by BAPV module designers and installers.

To my Father, Mother and Parents-in-law

To my beloved wife

To my son, Daniel

ACKNOWLEDGMENTS

First and foremost, my utmost gratitude goes to Dr. Govindasamy Tamizhmani, whose sincerity and encouragement I will never forget. He served as an inspiration as I hurdled all of the obstacles involved in the completion of this research work. I would like to thank Dr. Bradley R. Rogers and Dr. Narciso F. Macia, for their interest and valuable suggestions to improve this work.

I also would like to thank Joseph Kuitche and Kamerine Kroner of TÜ V Rheinland PTL for their support and help and all of TÜ V Rheinland PTL staff for supporting this work. The funding support of Salt River Project (SRP) is greatly appreciated as well.

Last, I would like to thank my colleagues in the Department of Engineering Technology and Arizona State University Photovoltaic Reliability Laboratory for their kind help to finish this work successfully.

TABLE OF CONTENTS

Page

CHAPTER Page

CHAPTER Page

LIST OF TABLES

Table Page

LIST OF FIGURES

Figure Page

Figure Page

CHAPTER 1

INTRODUCTION

1.1 Background

A photovoltaic (PV) module is a device that converts sunlight to electricity. It has been anticipated that PV modules will be one of the main sources of alternative energy in the future because they generate energy. PV modules have been used in many applications, such as calculators, cars, power plants, and houses.

The Building Applied Photovoltaic (BAPV) system, also known as the Building Integrated Photovoltaic (BIPV) system or Rooftop Photovoltaic system, is a major application of the PV modules. The BAPV system is used mainly for residential and commercial application purposes. The BAPV systems have several advantages. First, a BAPV system does not requires dedicated land space because they are installed on the roof, unlike a commercial PV power plant. Every house has a roof, and most of them are available for harvesting sunlight. This means that every house has the space required to install BAPV modules. Thus, they can be installed for any house. Also, the BAPV module system does not make the exterior of the house look bad. Generally, the BAPV modules are installed horizontally on the roof such that they are parallel to the surface of the roof, so they appear to be just a part of the roof.

The performance of PV modules depends primarily on temperature and solar irradiance, and one of the main factors that dictates the performance of PV modules is the operating temperature of the cells. The performance of PV

modules decreases as the temperature of the modules increases due to the negative temperature coefficient of power output. Generally, the degradation rate of performance of the PV modules is 0.5%/℃ for crystalline silicon technology and 0.2%/℃ for thin-film technology [1]. The temperature of PV modules is dictated by ambient conditions, such as irradiance, ambient temperature, wind speed, wind direction, and humidity. Based on field data acquired by Arizona State University's Photovoltaic Reliability Laboratory (ASU-PRL), the effects of wind direction and humidity on open, rack-mounted PV modules were found to be negligible [6].

In hot climatic conditions, such as those in Arizona, the BAPV module temperature can reach as high as 95℃ during the peak temperatures of summer. Considering a general 0.5%/℃ power drop for crystalline silicon modules, a performance drop of about 30% would be expected during the summer months because of the difference between rated temperature (25℃) and operating temperature (~90℃). When the BAPV modules are installed on a roof, there is an air gap between the modules and the surface of the roof. The temperature of the BAPV modules is affected directly by the size of this air gap, which, in turn, affects the performance of the BAPV modules. Therefore, it is necessary to determine the optimum air-gap size in order to appropriately design a BAPV system. In addition, temperature prediction is very important in order to determine expected power output from the modules.

In Arizona, the PV industry has been booming for the last couple of years. According to the Arizona Department of Commerce, in 2008, the number of

residents who used electricity generated by PV modules in their homes was more than 1600. Along with utility companies, state government and federal government have provided incentives for homeowners to install PV modules on their houses by allowing tax credits for the modules. Therefore, it is expected that many manufacturers and installers will enter the BAPV module industry, and the performances of the various BAPV modules will be a key factor in choosing a specific BAPV module and system for installation.

The focus of this study is to determine the optimum size of the air gap between the BAPV module and the rooftop that will allow the optimal operational temperature while giving appropriate consideration to electricity generation capacity and safety issues. Thus, this study provides guidance for BAPV module manufacturers and installers in terms of air gap sizes and their relationship to the operating temperatures of the modules.

1.2 Statement of the Problem

There are several thermal models for open, rack-mounted PV modules, but only a few thermal models, if not only one, is available for BAPV modules [15]. This thermal model for BAPV modules was based on the field data from ASU-PRL, which were acquired only for one month.

The installed nominal operating cell temperatures (INOCTs) of such modules were reported by Sandia National Laboratory in 1987 [9], but current PV modules are larger and have greater output power. Therefore, the INOCTs must be revalidated using current, commercial PV modules.

The main objective of this study is to conduct various temperature measurements and tests of BAPV modules at a variety of ambient conditions in order to provide guidance about the effects of the operating temperatures on electricity generation and safety.

1.3 Scope of the Work

The scope of the work included:

- Collecting and monitoring ambient condition data [11] and collecting and monitoring temperature data for BAPV modules with various air gap sizes (0, 1, 2, 3, and 4inches) for a one-year period (May 2009 - April 2010).
- Installing five crystalline silicon 0-inch air gap modules with backsides covered with R30 insulation materials.
- Developing mathematical models for the prediction of the temperatures of BAPV modules and back-insulated modules.
- Measuring and predicting the nominal operating cell temperatures (NOCTs) of BAPV modules and back-insulated modules.
- Analyzing the temperature test data in accordance with safety standards, which have been tested by TÜ V Rheinland PTL (formerly ASU-PTL) [10].

1.4 Limitations

The mock roof construction is limited to only one pitch and one type of roof tile, which is cement-based concrete. Even though the 0-inch air gap modules stick to the surface of the roof, stagnant air still exists below the modules due to space between the laminate of the module and the tile. Thus, the modules for which the backsides were covered with insulation material were used for 0-inch

air gap situations, which could be considered as the worst-case condition. The thermal models developed in this work and the INOCTs are limited to crystalline silicon modules with glass superstrates and polymeric substrates.

CHAPTER 2

LITERATURE REVIEW

2.1 Energy Model

The energy output of common generators is acquired by integrating with time; however the power performance of a PV module depends on many factors, such as module temperature, irradiance, spectral response of the module, and characteristics of the module itself. Generally, the energy is calculated from the daily power production by numerical integration according to the equation below [3]:

$$E = \Delta t \times \sum_{i=1}^{n} P_i$$

where:

E: module output energy (Wh);

Δt: data sampling interval (hours);

P_i: power at the i^{th} sample time (W).

2.2 Temperature Coefficients

The temperature coefficient is used to determine the effect of temperature on the output voltage, output current, or output power of a PV module. Due to the physical characteristics of silicon, the output power from a crystalline silicon PV cell decreases as the temperature of the cell increases, and a typical temperature coefficient of output power for a crystalline silicon PV cell is -0.5%/°C [1]. Therefore, the temperature coefficient is used as a parameter, along with the PV module's voltage, current, and power, for determining the performance of the PV

module. Generally, the temperature coefficients for insulated-back PV modules are lower than those for open-rack PV modules, as shown in Figure 2.1 [2]. This is probably because of more uniform distribution of temperature throughout the module.

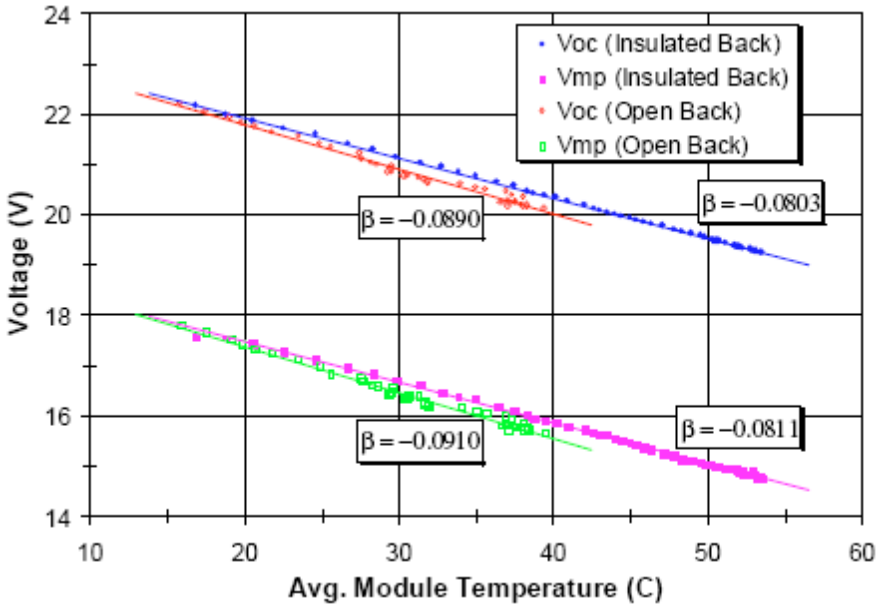

Figure 2.1 Measured temperature coefficients for voltage of a 36-cell c-Si module measured outdoors, with and without back-surface thermal insulation [2]

2.3 Thermal Model

The temperature a PV module is related directly to the power output of the module due to the intrinsic characteristics of silicon. The temperature of the module also depends on various factors, such as ambient conditions (irradiance, wind speed, wind direction, relative humidity, and ambient temperature), module installation (open-rack or roof-mounted), and the characteristics of the module itself. Several thermal models have been developed in the past. They were

obtained from either field data or a theoretical heat balance approach. In this section, several thermal models are reviewed.

2.3.1 Simple Model

The simple model was based on the fact that the operating temperature of solar cells above ambient is roughly proportional to the irradiance when the module is mounted on the open rack and wind speed is low [4].

$T_{cell} = T_{ambient} + 0.031 \times \text{Irradiance}$

where:

T_{cell}: solar cell temperature (℃);

$T_{ambient}$: ambient temperature (℃);

Irradiance: solar irradiance (W/m^2).

2.3.2 NOCT Model

For an open-rack mounted system with low wind speed, the temperature of the module temperature can be calculated as a function of irradiance and ambient temperature based on the module's nominal operating cell temperature (NOCT). The NOCT model equation is given below [5].

$$T_{module} = T_{ambient} + (T_{NOCT} - 20) \times \frac{\text{Irradiance}}{800}$$

where:

T_{module}: module temperature (℃);

$T_{ambient}$: ambient temperature (℃);

T_{NOCT}: nominal operating cell temperature, NOCT (℃), of the module;

Irradiance: solar irradiance (W/m^2).

2.3.3 IEC 61853 Model

The IEC 61853 draft standard has a thermal model based on a consensus basis. This fits a specific windspeed range [7].

$$T_{module} - T_{ambient} = b \times G + a$$

where:

T_{module}: module temperature (℃);

$T_{ambient}$: ambient temperature (℃);

a, b: coefficients for a certain wind speed range;

G: irradiance (W/m^2).

2.3.4 Tang's Model

Yingtang Tang's Master's thesis, "Outdoor Energy Rating Measurements of Photovoltaic Modules," was followed as a model for predicting the temperature of a PV module in an open-rack PV system with respect to ambient conditions. This model is used in predicting the temperature of the PV module for large, open-rack PV systems. Three thermal models were presented in the research performed by Tang [6].

Tang's thermal model is shown in the equation below. Five input parameters are used in this model.

$$T_{module} = w_1 \times T_{amb} + w_2 \times E + w_3 \times \mathrm{WindSpd} + w_4 \times \mathrm{WindDir} + w_5 \times \mathrm{Humidity} + c$$

where:

T_{module}: module temperature (℃);

T_{amb}: ambient temperature (℃);

E: irradiance (W/m^2);

WindSpd: wind speed (m/s);

WindDir: wind direction (°);

Humidity: relative humidity (%);

w_1 - w_5: coefficients;

c: constant.

The output results from the equation showed that ambient temperature is a major factor that increases the module temperature. Irradiance and wind speed also affect the temperature of the module, although not to the same extent as ambient temperature. However, the effects of wind direction and relative humidity are almost negligible, so there is also a second thermal model in his thesis that does not include wind direction and relative humidity.

The second thermal model is given in the equation below, and three input parameters are used.

$$T_{module} = w_1 \times T_{amb} + w_2 \times E + w_3 \times WindSpd + c$$

where:

T_{module}: module temperature (℃);

T_{amb}: ambient temperature (℃);

E: irradiance (W/m^2);

WindSpd: wind speed (m/s);

w_1 - w_3: coefficients;

c: constant.

The overall average of each coefficient from field experimental data is shown in the table below.

Table 2.1 Overall average coefficients for open-rack PV modules

	w_1	w_2	w_3	c
Overall average	0.943	0.028	-1.528	4.328

The third thermal model has the format shown in the equation below, in which there are two input parameters, i.e., ambient temperature and irradiance. The interval of wind speed is 0.5 m/s.

$T_{module} - T_{amb} = m \times E + b$

where:

T_{module}: module temperature (℃);

T_{amb}: ambient temperature (℃);

E: global solar irradiance (W/m^2);

m and b are coefficients.

The coefficients for each module are acquired from the field data. Coefficients b and m typically range from 0.5 - 1.5 and 0.0054 - 0.0094 at wind speeds of 0.25 - 9.25 m/s, respectively, based on the field data.

Several models were presented in this chapter, and the thermal models among them are mainly the ones that are useful for this work. The temperature prediction equation of this project is also based on field data, and a mathematical model similar to Tang's model was generated for the BAPV system in this project.

2.4 Standards Regarding Temperature of PV modules

Several temperature measurements of PV modules have been conducted in accordance with IEC 61215, IEC 61730-2, and UL 1703 standards that complement the Standard Test Condition (STC), which is not representative of the real conditions that PV modules experience when they are operating in the field. Two such measurements are the nominal operating cell temperature (NOCT), described in the IEC 61215 standard, and the Temperature Test found in IEC 61730-2 and in the UL 1703 safety standard [12, 13, 14].

2.4.1 Measurement of NOCT – IEC 61215

The output power of the PV module is dependent on the temperature of the module due to its intrinsic characteristics. Manufacturers of PV modules use performance measurements recorded at STC to rate their modules for market use. The STC assumes that the operating temperature of the module is maintained at 25℃. However, in reality, it is rare that PV modules are operated at STC. Thus, NOCT has been added to the standard, and manufacturers should provide both the module temperature at STC and NOCT. The IEC 61215 standard provides a procedure for the measurement of NOCT [12]. The NOCT is defined as the equilibrium average cell temperature with an open-rack mounted module at the following Standard Reference Environment (SRE) according to the IEC standard. Table 2.2 shows the SRE for NOCT, and the NOCT thermal model equation was presented in the previous section.

Table 2.2 Standard Reference Environment of NOCT

Tilt angle	45° from the horizontal
Irradiance	800 W/m^2
Ambient Temperature	20℃
Wind speed	1 m/s
Electrical load	None (open circuit)

2.4.2 Temperature Test – IEC 61730 and ANSI/UL 1703

A typical PV module is made of several components, including glass superstrate, polymeric encapsulant, solar cells, polymeric substrate/backsheet, a junction box, bypass diodes, and cables/connectors. The operating temperatures of these module components are determined primarily by the mounting configurations (e.g., open-rack and rooftop), electrical termination conditions (e.g., open-circuit, short-circuit, loaded), shading conditions (partial or full shading of solar cells), solar cell stringing configurations (number of cells in a string per bypass diode), and types of PV cells (low- or high-shunt PV cells). Both international (IEC 61730-2) and United States (UL 1703) safety standards require that the components in end-product, packaged PV modules be temperature tested [13, 14]. These standards provide procedures to determine the maximum reference temperatures of the various components of a PV module.

Chapter 3

METHODOLOGY

3.1 Temperature Prediction of BAPV Modules

The prediction of the temperatures of BAPV modules is based on field data acquired under natural sunlight with outdoor controlled equipment. The temperatures of the modules in the field were monitored for a one-year period, and, then, thermal models were developed based on the field data. Details about the methodology of monitoring the temperatures of the modules in the field and developing mathematical model are presented in this chapter.

3.1.1 BAPV Module Installation

In order to install the BAPV modules, a mock roof was designed and constructed at Arizona State University's Photovoltaic Reliability Laboratory (ASU-PRL) in Mesa, Arizona. The specifications of the mock roof are detailed below.

- Roof dimension: 32 x 17.5 ft
- Roof orientation: South fixed
- Roof pitch: 23° from horizontal
- Roofing materials: cement based concrete flat tiles
- Air gap spacing: 0, 1, 2, 3, and 4 inches

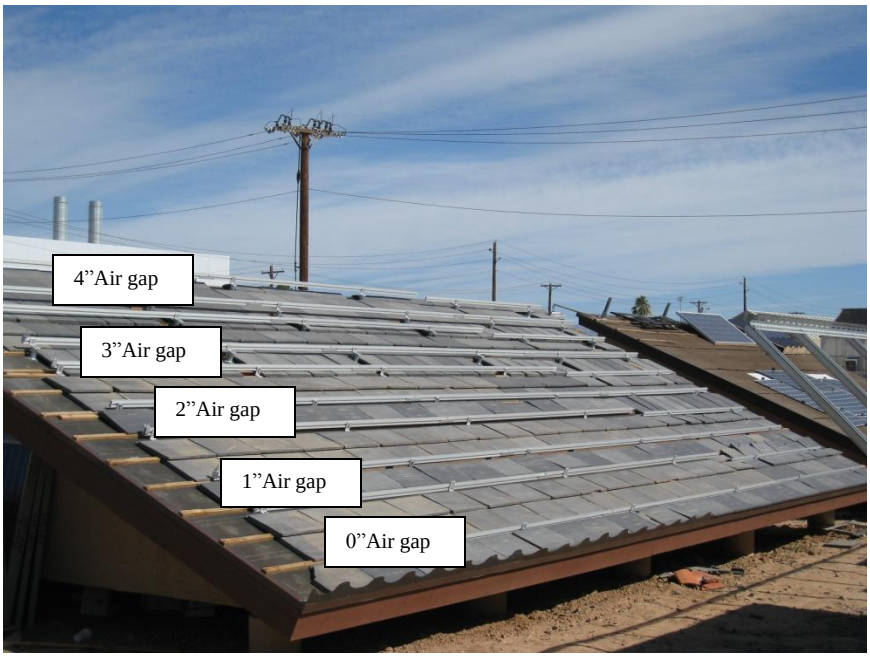

Figure 3.1 Mock roof with different air gaps

Twenty PV modules from four different manufacturers were selected for use in monitoring the temperatures of the BAPV modules. Crystalline silicon technology PV modules were chosen for this experiment. Ten BAPV modules were from two different manufacturers that used poly crystalline silicon (poly c-Si) technology, and the other 10 BAPV modules were from two different manufacturers that used mono crystalline silicon (mono c-Si) technology. The array configurations are detailed below, in Table 3.1 and Figure 3.1.

- Test technology: poly c-Si and mono c-Si
- Module electrical termination: open-circuit
- Number of test modules: 20 (10 mono c-Si; 10 poly c-Si)
- Array matrix: 4 columns (5 modules each) x 5 rows (4 modules each)
    - Column 1: poly c-Si BAPV modules [manufacturer 1]
    - Column 2: mono c-Si BAPV modules [manufacturer 2]

- Column 3: poly c-Si BAPV modules [manufacturer 3]
- Column 4: mono c-Si BAPV modules [manufacturer 4]
- Row 1: 0” air gap (0 cm air gap)
- Row 2: 1” air gap (2.54 cm air gap)
- Row 3: 2” air gap (5.08 cm air gap)
- Row 4: 3” air gap (7.62 cm air gap)
- Row 5: 4” air gap (10.16 cm air gap)

- Distance between modules in each column: 2 – 6 in (5 - 15 cm)
- Distance between modules in each row: 1 in (2.54 cm)
- Depth of module frame. ~2 in (5 cm)

Table 3.1 Array of BAPV modules on the mock roof

	Roof top			
	Column 1	**Column 2**	**Column 3**	**Column 4**
4” air gap	Poly c-Si	Mono c-Si	Poly c-Si	Mono c-Si
3” air gap	Poly c-Si	Mono c-Si	Poly c-Si	Mono c-Si
2” air gap	Poly c-Si	Mono c-Si	Poly c-Si	Mono c-Si
1” air gap	Poly c-Si	Mono c-Si	Poly c-Si	Mono c-Si
0” air gap	Poly c-Si	Mono c-Si	Poly c-Si	Mono c-Si
	Roof bottom			

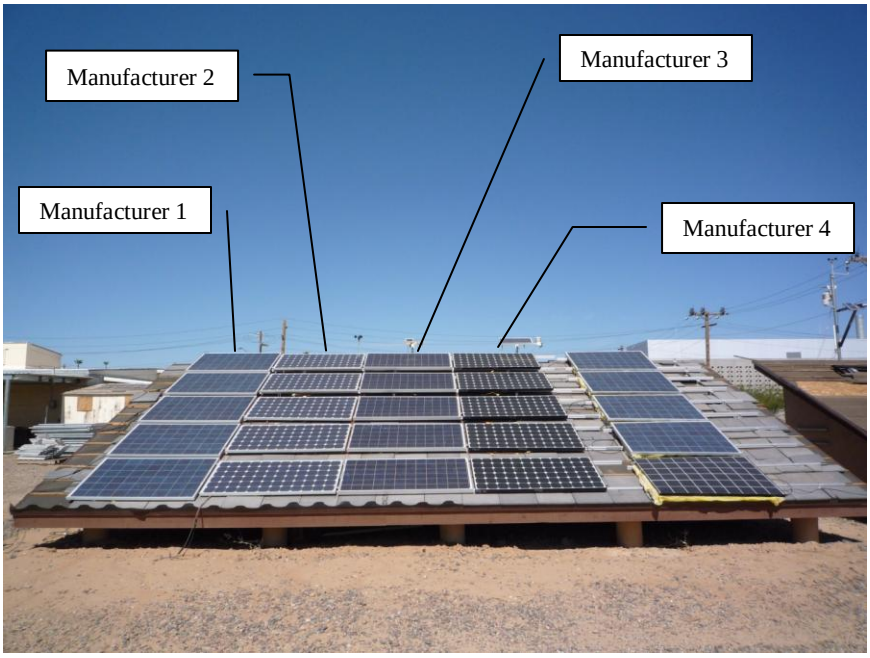

Figure 3.2 Array of BAPV modules on the simulated rooftop structure

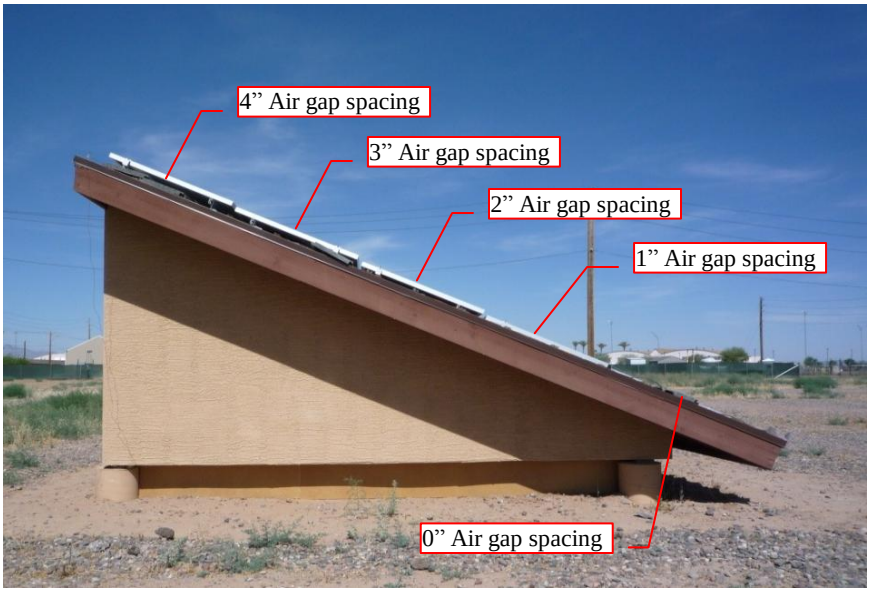

Figure 3.3 Side view of the simulated rooftop structure with installed modules

3.1.2 Preparation of BAPV Modules

BAPV modules from different manufacturers were chosen for a one-year period of field monitoring. The electrical specifications of these modules are given in Table 3.2.

Table 3.2 Electrical specifications for the BAPV modules from four manufacturers

	Electrical specification				
Manufacturer/Column	**I_{sc} (A)**	**V_{oc} (V)**	**I_{mp} (A)**	**V_{mp} (V)**	**P_{max} (W)**
# 1	7.89	33.0	7.31	26.0	190.1
# 2	7.78	31.6	7.23	23.5	169.9
# 3	5.20	44.3	4.80	35.6	170.9
# 4	5.90	47.8	5.50	40.0	220.0

Two cells of each BAPV module were selected for monitoring the module temperature. The procedure for selecting the cells and attaching the thermocouples was same as NOCT test module preparation. The two cells were located in the middle of the BAPV module. The backsheet of the cells were cut in order to access the encapsulated cells, and a K-type thermocouple was attached to each cell with thermally conductive paste. The cells with the attached thermocouples were sealed with thermal tape to avoid exposing the cells to moisture.

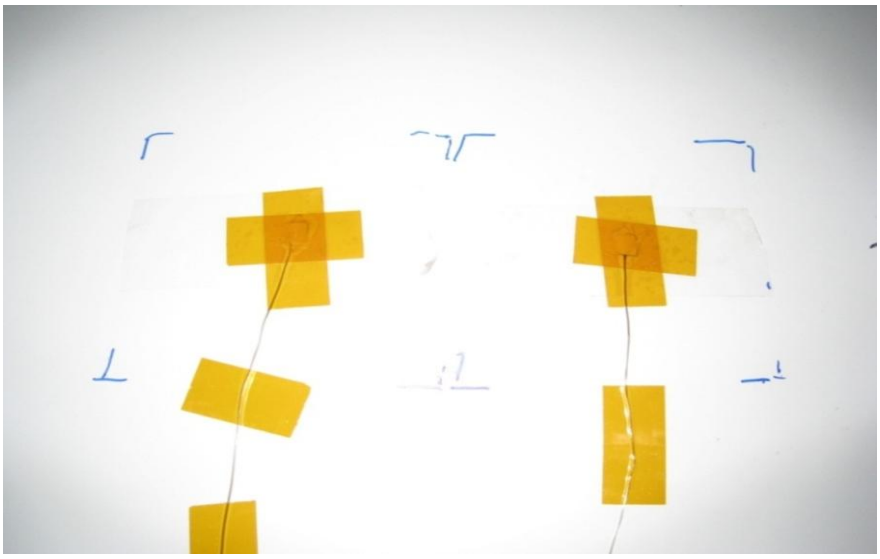

Figure 3.4 K-type thermocouple sealed with thermal tape inside cut cell

3.1.3 Measurement of Air-Gap Temperature

The corresponding air-gap temperatures were measured while the module temperatures at the different air gaps (0”, 1”, 2”, 3”, and 4”) were measured. Twenty K-type thermocouples were fixed under each BAPV module between the tiles. The location of the air-gap thermocouple is shown in Figure 3.5.

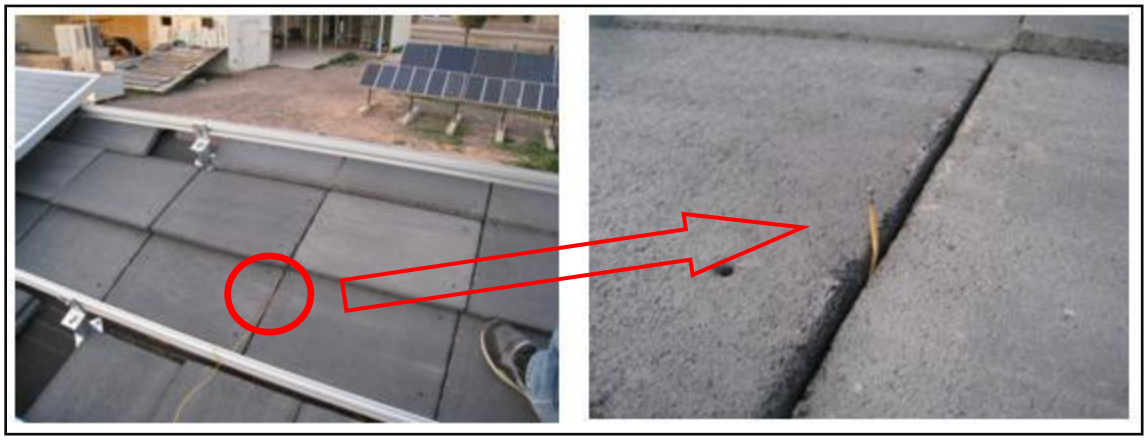

Figure 3.5 K-type thermocouple to measure air temperature of the corresponding air gap between the module and the tile roof

In addition to measuring module temperature with different air gaps and air gap temperatures, the tile temperatures were measured at the portions exposed to the sun and the portions shaded by the BAPV module. For measuring the temperature of the tile, the tile next to the BAPV module was selected, and the thermocouple was placed on the tile. The other thermocouple was placed on the surface of the tile below the BAPV module.

3.1.4 Measurement of Ambient Conditions

In this project, ambient conditions (irradiance, ambient temperature, wind speed, and wind direction) are very important for predicting the temperatures of the modules. In order to measure irradiance, an EKO pyranometer was installed on the roof with the same pitch as the mock roof. For verifying the accuracy of the measured irradiance, the Energy Environmental Technology Service (EETS) reference cell also was installed on the roof. Both the pyranometer and the reference cell were fixed on the wooden plate that has same tilt angle as the roof.

The ambient temperature, wind speed, and wind direction were measured from the weather station next to the mock roof.

3.1.5 Data Acquisition System

Obviously, a data acquisition system (DAS) was necessary to collect the extensive quantity of temperature data over the one-year period. For the data collection, a National Instruments data acquisition system was installed behind the mock roof. The four NI-9211 modules that were connected to the thermocouples were hard wired to the high-speed, USB DAS, which was

controlled by the LabVIEW signal express program, which is a powerful and flexible graphical development environment created by National Instruments, Inc.

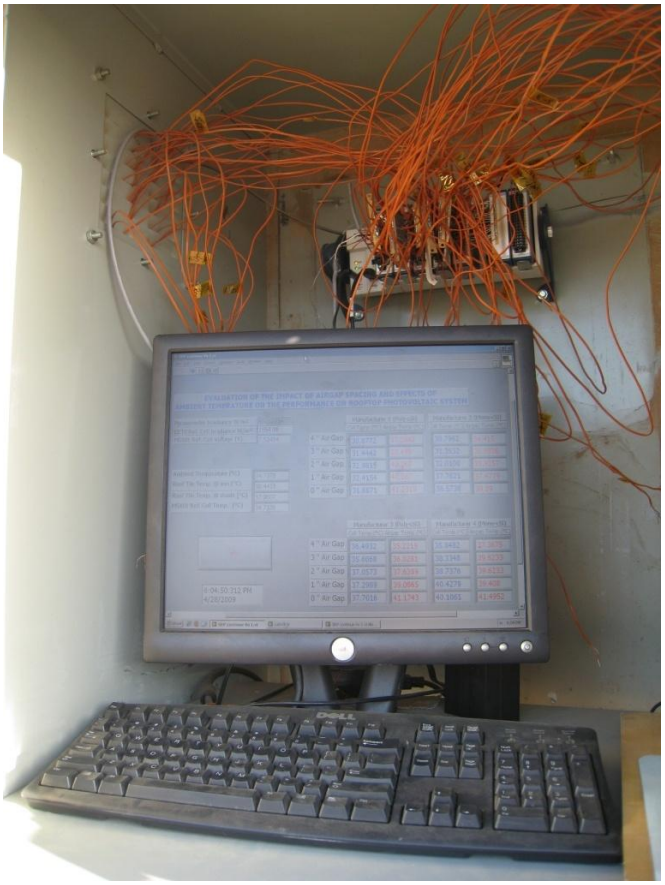

Figure 3.6 NI-9172 high speed USB DAS controlled by LabVIEW signal express program code

The LabVIEW program code for this DAS was created mainly by a former student who started this project, and minor changes were made to the code to accommodate additional BAPV modules. The LabVIEW program has a front panel that shows the current temperatures of all the components, as well as the irradiance measured by the EKO pyranometer and the EETS reference cell. A screenshot of the front panel is shown in Figure 3.7.

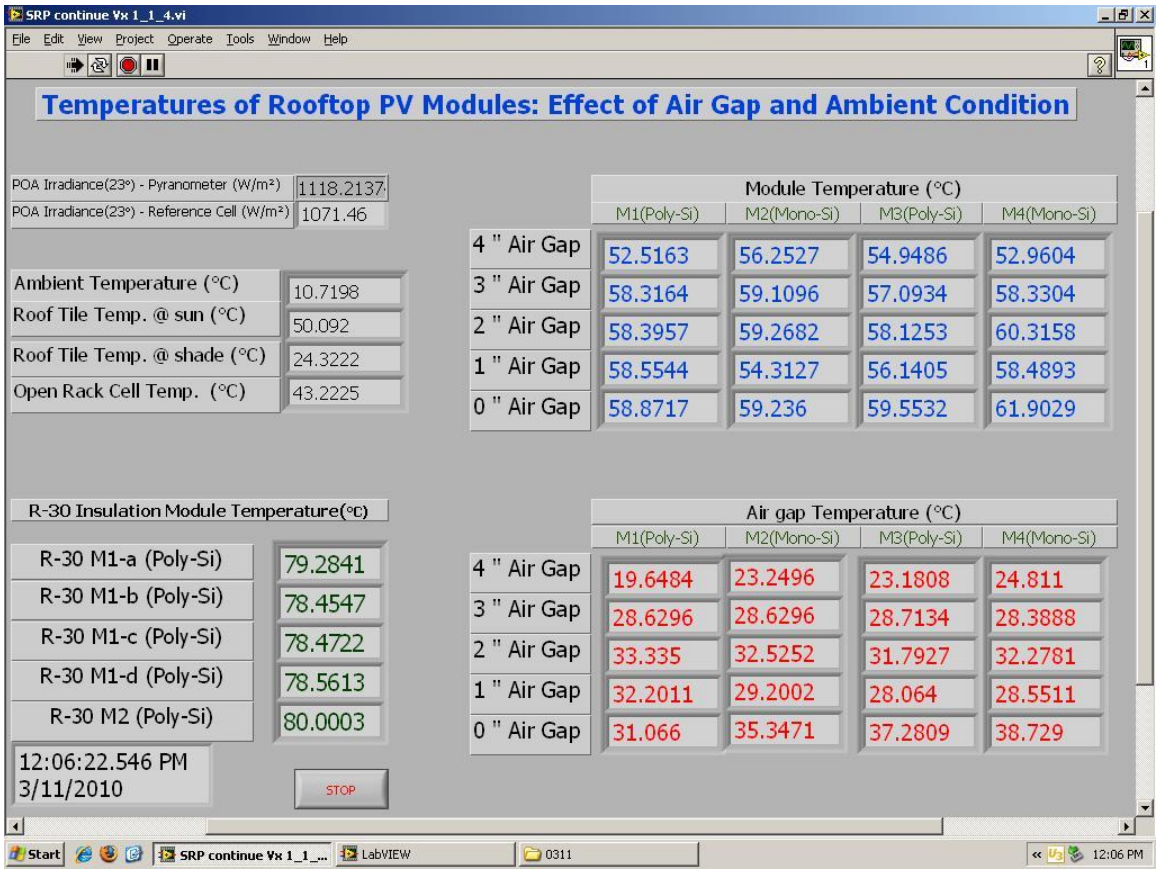

Figure 3.7 Front panel of LabVIEW, showing real time readings of parameters

3.2 Temperature Prediction for Back-Insulated BAPV Modules

While temperature predictions for BAPV modules were required to determine the air gaps that produced the best performance, temperature predictions for the back-insulated BAPV modules were used to ensure the safety of the BAPV modules. The maximum temperature of the BAPV module in the worst-case condition must be known in order to prevent any safety hazard, such as fire.

3.2.1 Preparation and Installation of Back-Insulated BAPV Modules

In order to get the maximum temperature of the BAPV modules, the backside of the modules must be covered perfectly to minimize the temperature-

lowering effect of wind. Five poly c-Si modules were selected for this project, and their specifications are shown in the Table 3.3.

Table 3.3 Electrical specifications of BAPV modules from two manufacturers

	Electrical Specification				
Manufacturer	**I_{sc} (A)**	**V_{oc} (V)**	**I_{mp} (A)**	**V_{mp} (V)**	**P_{max} (W)**
# 1 (4 modules)	7.89	33.0	7.31	26.0	190.1
# 2 (1 modules)	7.80	32.6	7.30	25.5	186.2

R-30 insulation material (~23cm-thick fiberglass insulator) was attached to the backsides of the modules. One K-type thermocouple for one BAPV module was attached with a conductive paste to the middle cell that was cut to allow the installation of the thermocouple. The space between the frame and the substrate was filled with insulation (shown in Figure 3.8), and, then, all of the substrate was covered with the insulation material, as shown in Figure 3.9.

Figure 3.8 Before covering the BAPV reference module with insulation material

Figure 3.9 After covering the BAPV reference module with insulation material

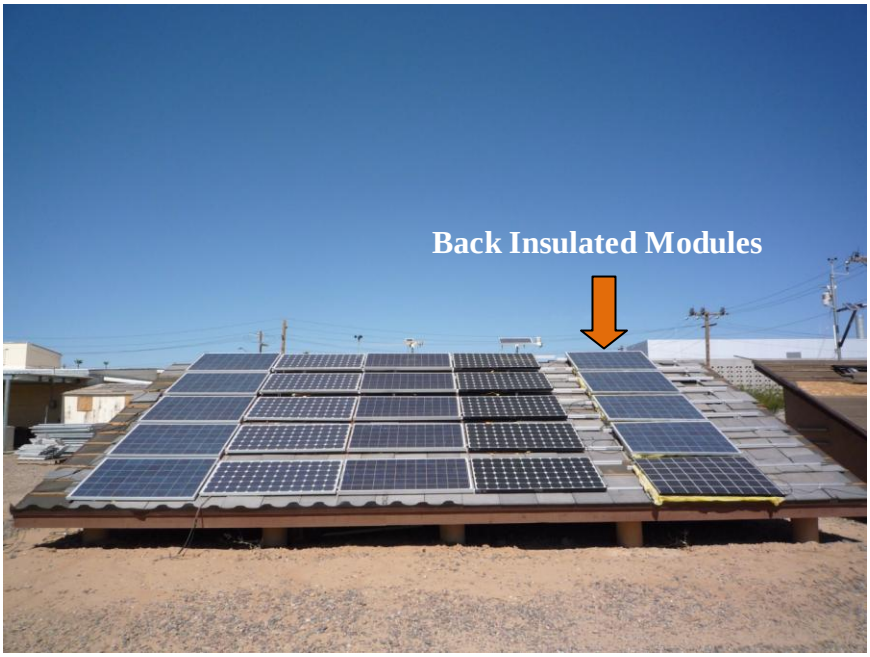

Figure 3.10 BAPV Modules on the Mock Roof

All five back-insulated BAPV modules were installed on the same mock roof, and they did not have any air gap between the backside of the module and

the surface of the roof. Each thermocouple was connected to the DAS behind the roof and monitored for maximum temperature.

3.2.2 Measurement of Ambient Conditions and the DAS

The back-insulated BAPV modules were installed on the same mock roof, thus the same weather station data were used for this experiment. The weather station collected ambient temperature, wind speed, and wind direction.

The same DAS was used to collect the temperatures of the back-insulated BAPV modules, so that the DAS was able to collect the temperature of every module simultaneously. Five channels from the National Instrument module were assigned to collect the temperature of the five back-insulated BAPV modules.

3.3 Model Development

The objective of developing a thermal model was to analyze the temperature variation and its influence on the performances of the BAPV modules with different air gaps of 0”, 1”, 2”, 3”, and 4”, respectively, on the BAPV system with respect to ambient temperature and other influencing parameters, such as wind speed, wind direction, and solar irradiance. The method of linear regression was chosen for this work, and MATLAB was used for this mathematical model development. The results of the thermal model are presented in Chapter 4.

3.4 Measurement and Prediction of INOCT for BAPV modules and Back-Insulated PV modules

The measurement of installed NOCT (INOCT) of BAPV modules and back-insulated PV modules was based on the method in the IEC 61215 standard. The measurement of INOCT followed the standards as closely as possible. There

were a few things in the standard that could not be followed due to the limitations imposed by the test conditions, which are shown in Table 3.4. One good day, which means constant irradiance with low wind speed, was selected for obtaining the INOCT. Temperature data were collected from 10:00 A.M. to 3:00 P.M. at six-minute intervals.

Table 3.4 Difference between NOCT and INOCT in this study

	Required NOCT standard test conditions	**INOCT in this study test conditions**
Tilt Angle	45°±5°	23°
Mount	Open-rack	Different air gap spacing or insulated
Around module	The modules of same design with no space among modules	The modules of same design are in the same column with different space depending on column and row.
Data collection interval	No more than 5 seconds	Every 6 minutes

3.5 Temperature Test

The temperature test results of approximately 140 crystalline silicon modules from various module manufacturers tested at TÜ V Rheinland PTL (formerly, Arizona State University's Photovoltaic Testing Laboratory) between 2006 and 2009 were presented in Chapter 4. In this investigation, only the test results of the conventional crystalline silicon modules were presented and analyzed, excluding the thin-film modules, double glass modules, and high efficiency mono crystalline silicon modules. The temperature tests were done under three different electrical termination conditions, i.e., open-circuit, short-circuit, and short-circuit with half shaded cell (hereafter called the shorted-shaded

configuration). The UL 1703 standard requires testing under all three of the termination conditions, whereas IEC 61730-2 does not require the shorted-shaded termination condition.

The test modules were prepared by attaching a large number of thermocouples to the specific components/locations. Table 3.5 shows the thermocouple locations that were used for the temperature tests.

Table 3.5 Nine thermocouple locations of various components during the temperature tests

Number	Test Location
1	Front glass[a]
2	Substrate[b]
3	Cell[c]
4	J-box ambient
5	J-box surface
6	Positive terminal
7	J-box backsheet
8	Field wiring
9-1	Diode 1
9-2	Diode 2
9-3	Diode 3

[a] Above center cell; above exposed portion of half-shaded cell for short-circuit & shaded condition

[b] Substrate under half-shaded portion of the cell during short-circuit & shaded condition

[c] Half-shaded portion of the cell during short-circuit & shaded condition. Backsheet was cut and resealed to place the thermocouple.

The monitored component temperatures were all normalized to 1000 W/m^2 irradiance, 40°C ambient temperature, and an average wind speed of 1 m/s, in accordance with the procedures of the safety standards. The normalized

temperature (in ℃) of each component was calculated using the following equation:

$$T_{norm} = (T_{max} - \text{Mean } T_{amb}) \times \frac{1000}{\text{Mean Irradiance}} + 40 \quad (3.1)$$

where:

T_{norm}: the normalized temperature;

T_{max}: the maximum component temperature during the test;

T_{amb}: the ambient temperature during the test.

The test standards [13, 14] may be referenced for the details of the required test set up, outdoor test conditions, and data acquisition system. The results are presented and discussed in Chapter 4 with three subsections, i.e., open-circuit condition; short-circuit condition; and shorted-shaded condition.

CHAPTER 4

RESULTS AND DISCUSSION

4.1 Thermal Modeling of BAPV Modules – Effect of Air Gap

Two types of mathematical thermal models for temperature prediction were developed, and they are presented in this section. One is for the overall BAPV array, and the other one is for the individual columns of the BAPV array. Both thermal models were developed with three input parameters, i.e., irradiance, ambient temperature, and wind speed.

4.1.1 Thermal Model for the overall BAPV array

Based on the data acquired in May 2009, a preliminary thermal model was developed and reported for crystalline silicon modules [8]. In this work, the data acquisition period was extended to one full year and a thermal model was developed. The thermal model used in this work is shown in equation (4.1) below.

$$T_{module} = w_1 \times E + w_2 \times T_{amb} + w_3 \times WS + c \quad (4.1)$$

where:

T_{module}: module temperature (℃);

E: irradiance (W/m^2);

T_{amb}: ambient temperature (℃);

WS: wind speed (m/s);

w_1- w_3: coefficients;

c: constant.

A linear regression fit to the data provides the required coefficients for the development of the thermal model, and the MATLAB program was used to

extract these coefficients. In order to determine whether the short-term coefficients and long-term coefficients are independent of testing period/season, the coefficients obtained with one-month data (May 2009; monthly coefficients) and one-year data (May 2009 - April 2010; annual coefficients) were compared. A comparison of these coefficients is shown in Table 4.1 (wide wind speed range of up to 4 m/s) and Table 4.2 (narrow wind speed range of up to 2 m/s). For this comparison, only the averages of column 2 and column 3 coefficients were considered. These tables clearly indicate a considerable influence of the testing period (one month vs. one year) on the extent of these coefficients (or on the significance levels). Therefore, it was decided to develop the coefficients for all the four seasons (seasonal coefficients) of a year, and they are presented in Appendix A.

Table 4.1 Comparison of one-month and one-year thermal model coefficients of the entire array for a wide wind speed range (up to 4 m/s)

	Coefficients based on 1-month data				Coefficients based on 1-year data			
Air Gap	Irradiance (w_1)	T_{amb} (w_2)	Wind Speed (w_3)	Const.	Irradiance (w_1)	T_{amb}(w_2)	Wind Speed (w_3)	Const.
0”	0.040	1.27	-1.01	-6.38	0.033	1.08	-2.02	8.06
1”	0.037	1.21	-0.98	-4.28	0.031	1.10	-1.96	7.00
2”	0.036	1.10	-1.08	-3.88	0.034	0.87	-2.43	11.20
3”	0.035	1.03	-1.41	-1.37	0.032	0.85	-3.18	12.84
4”	0.031	1.09	-1.69	-2.18	0.030	0.84	-3.56	12.86

Table 4.2 Comparison of one-month and one-year thermal model coefficients of the entire array for narrow wind speed range (up to 2 m/s)

	Coefficients based on 1-month data				Coefficients based on 1-year data			
Air Gap	Irradiance (w_1)	T_{amb} (w_2)	Wind Speed (w_3)	Const.	Irradiance (w_1)	T_{amb} (w_2)	Wind Speed (w_3)	Const.
0”	0.040	1.20	-0.06	-4.97	0.035	1.03	-0.21	5.47
1”	0.037	1.14	-0.20	-2.93	0.032	1.06	-0.49	4.81
2”	0.036	1.03	-0.43	-2.22	0.036	0.82	-0.96	9.00
3”	0.035	0.96	-1.00	0.48	0.035	0.79	-2.13	10.73
4”	0.031	1.02	-1.19	-0.45	0.033	0.78	-2.94	11.11

4.1.2 Thermal Model for individual columns of the BAPV array

In a previous study related to this topic [8], it was indicated that the wind direction also plays a significant role on the temperatures of the BAPV modules. Figure 4.1 shows a real-time screenshot of the front panel of the LabVIEW program, and it clearly shows that wind direction has a significant influence on the temperatures of the modules, depending on whether they are located at the center or edges of the array. Two options were considered to incorporate the effect of wind direction on the temperatures of the modules, i.e., (i) develop a four-parameter model (irradiance, ambient temperature, wind speed, and wind direction) instead of a three-parameter model (irradiance, ambient temperature, and wind speed) and (ii) develop a three-parameter model for every column of the array rather than for the entire array. For the sake of simplicity, it was decided to exercise the second option. Based on the one-year data, the coefficients of the three-parameter thermal model for the individual columns were developed, and they are presented in Table 4.3. The seasonal and monthly breakdowns of these coefficients for the individual columns of the array are provided in Appendix A

and B respectively. Due to time constraints, Appendix B includes monthly coefficients only for the column 3 modules. An example correlating the predicted temperature with the actual temperature for the column 3 - air gap 3 modules for the winter of 2009-2010 is presented in Figure 4.2. For the sake of simplicity, the linear regression model shown in Equation 4.1 was developed; however, the non-linear influence of wind speed and thermal radiation on the thermal model will be addressed in a future publication.

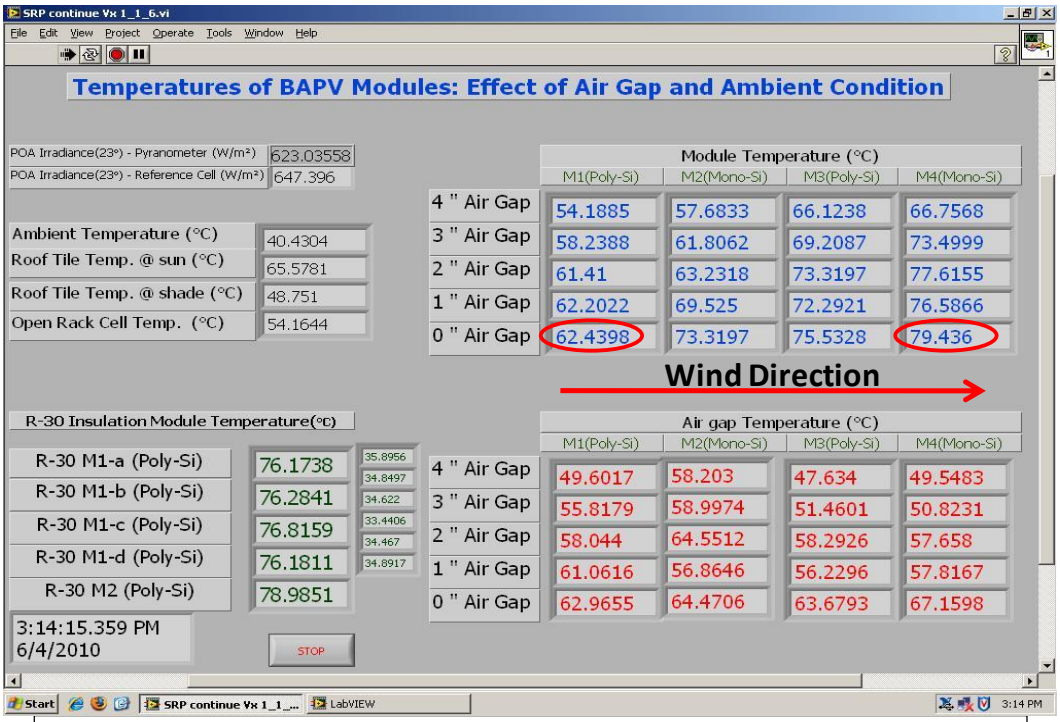

Figure 4.1 Real-time screenshot of front panel - effect of wind direction on the temperatures of the PV modules

Table 4.3 Thermal model coefficients for the individual columns of the array based on one-year data

	Mnf 1/Column 1(Poly)				Mnf 2/Column 2(Mono)				Mnf 3/Column 3(Poly)				Mnf 4/Column 4(Mono)			
	Irr (w1)	T_{amb} (w2)	WS (w3)	Const	Irr (w1)	T_{amb} (w2)	WS (w3)	Const	Irr (w1)	T_{amb} (w2)	WS (w3)	Const	Irr (w1)	T_{amb} (w2)	WS (w3)	Const
4inch	0.029	0.66	-2.99	14.93	0.030	0.64	-3.08	15.35	0.029	1.02	-3.12	9.95	0.027	1.06	-3.07	9.67
3inch	0.032	0.69	-2.85	14.45	0.032	0.67	-2.75	15.66	0.031	1.02	-2.85	9.90	0.030	1.10	-2.89	10.77
2inch	0.033	0.72	-2.53	13.09	0.034	0.70	-2.27	14.02	0.033	1.05	-2.20	8.80	0.032	1.12	-2.34	10.05
1inch	0.033	0.74	-2.31	12.78	0.030	1.09	-1.78	7.00	0.032	1.10	-1.91	7.16	0.032	1.10	-2.02	9.35
0inch	0.034	0.74	-2.02	12.44	0.033	1.08	-1.94	7.92	0.033	1.08	-1.89	8.09	0.033	1.17	-2.16	8.69

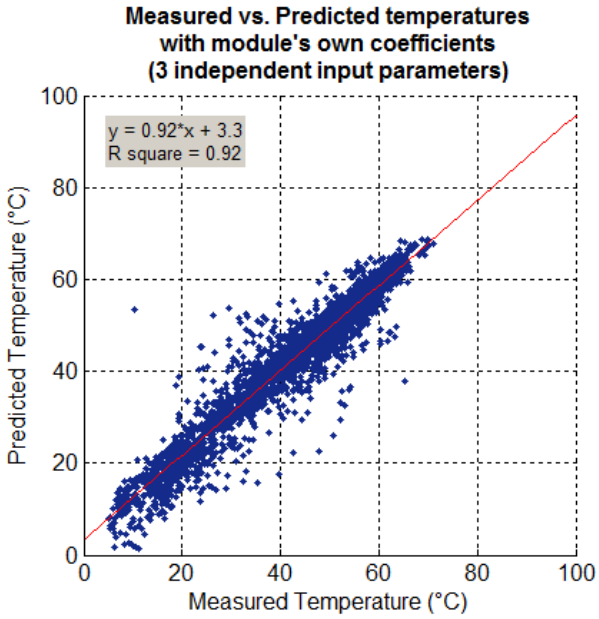

Figure 4.2 Linear correlation between predicted and measured temperatures for the winter of 2009-2010 (Column 3 modules; Air gap = 3 inches)

The combined effect of air gap and column (module location on the roof) on individual coefficients is presented in a three-dimensional plot shown in Figures 4.3, 4.4, 4.5, and 4.6. From these figures, the following observations can be made:

- Irradiance coefficient: It generally increases as the air gap decreases irrespective of the column number.

- Wind speed coefficient: The wind speed effect generally increases as the air gap increases irrespective of the column number.
- T_{amb} coefficient: It generally remains the same as the air gap increases but it is typically lower for the first two columns compared to the last columns.
- Constant: It generally remains the same as the air gap increases but it is typically higher for the first two columns compared to the last columns.

It seems that there is an inter-adjustment between "T_{amb} coefficient" and the "constant" due to the influence of wind direction. The wind direction apparently has opposite effects on the "T_{amb} coefficient" and the "constant," whereas it has no effect on the "irradiance coefficient" and "wind speed coefficient." In other words, if the wind direction decreases the value of "T_{amb} coefficient," then it increases the value of "constant" without affecting the other two coefficients. A large deviation of the "constant" from zero and a large deviation of the "T_{amb} coefficient" from the typical value of one are good indicators of the disproportionate effect of wind direction on the temperatures of the modules. This observation appears to suggest that it may be necessary to mount the BAPV modules in the middle of the roof so that the issue of temperature non-uniformity between the modules can be minimized. Reducing the temperature non-uniformity reduces voltage variations between the modules and improves the overall performance of the array.

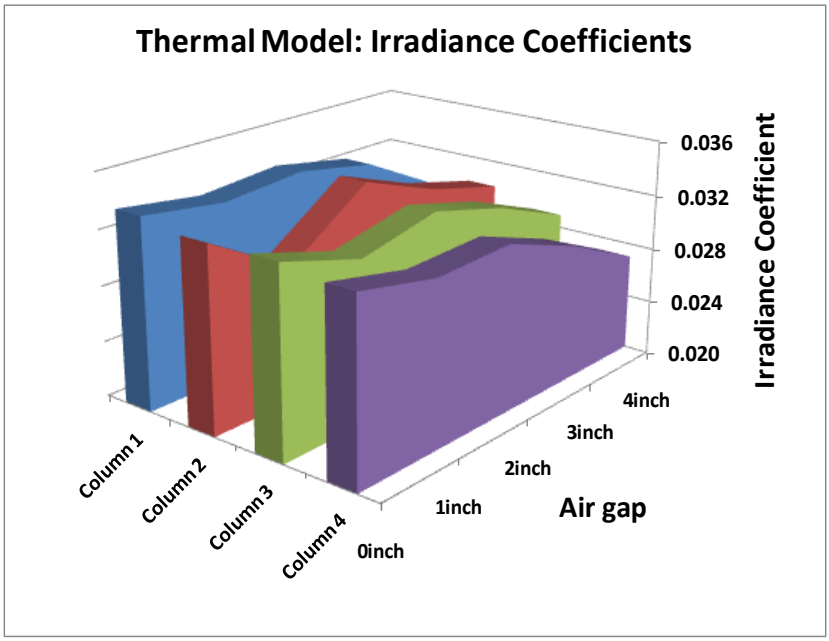

Figure 4.3 Effect of air gap and module column on the thermal model irradiance coefficients obtained based on one-year BAPV data

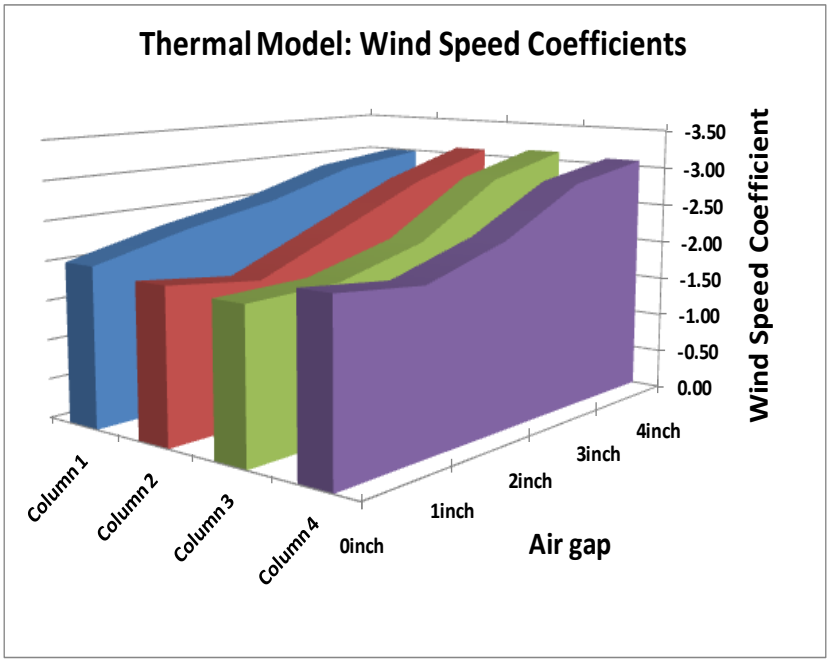

Figure 4.4 Effect of air gap and module column on the wind speed coefficients of the thermal model based on one-year BAPV data

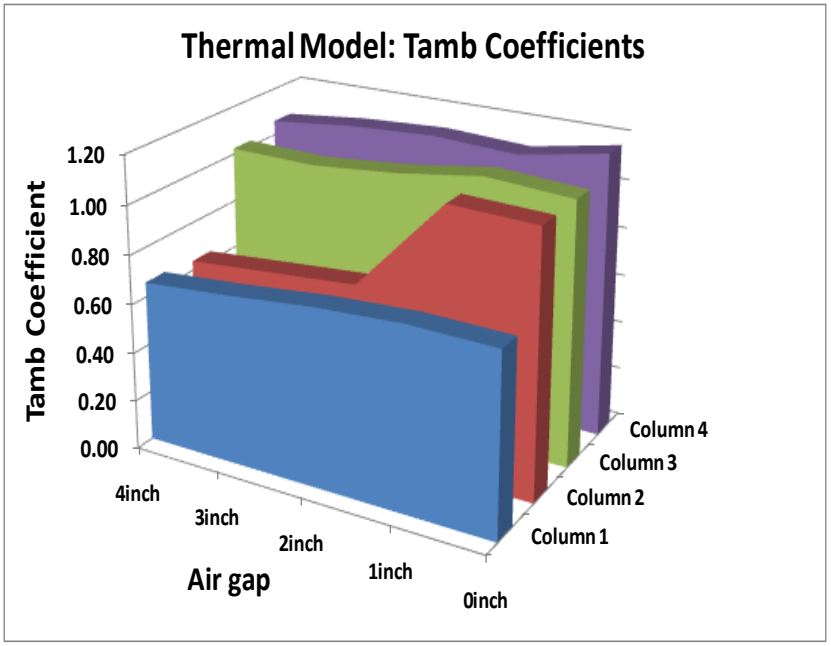

Figure 4.5 Effect of air gap and module column on the ambient temperature coefficients of the thermal model based on one-year BAPV data

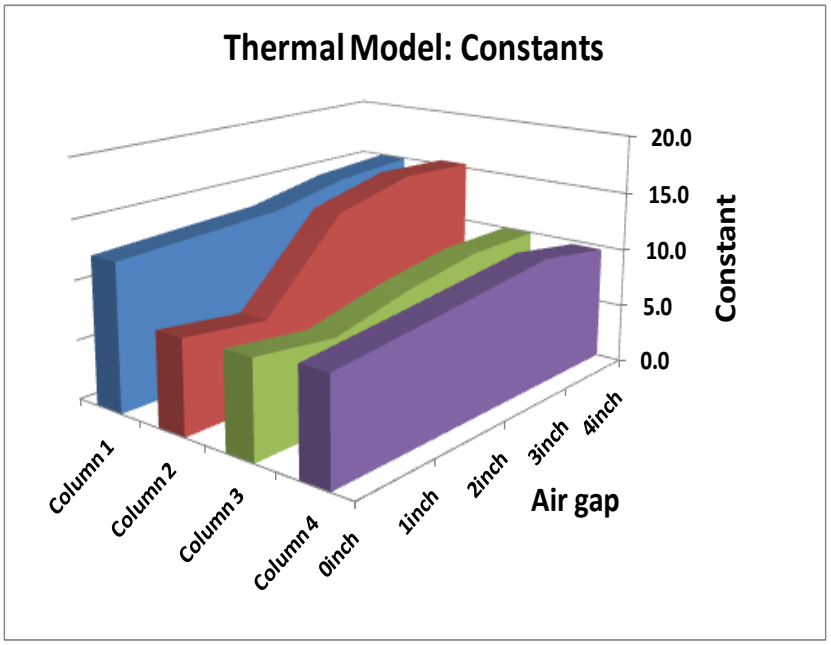

Figure 4.6 Effect of air gap and module column on the constant of the thermal model based on one-year BAPV data

4.2 Thermal Modeling of Back-Insulated BAPV Modules

In order to obtain a thermal model for the worst-case temperature scenario, the backsides of five modules (R30-1, R30-2, R30-3, R30-4, and R30-5) were insulated using R30 insulation foam, as shown in Figure 3.9. A thermal model was developed for these thermally back-insulated modules based on the data collected over a six-month period (October 2009 - March 2010).

The highest module temperature and highest temperature difference (delta $T = T_{module}-T_{ambient}$) observed during this testing period are reported in Table 4.4. It is interesting to note that the highest delta T of about 66℃ was observed when the ambient temperature was 10℃ and irradiance was 1057 W/m^2. When the ambient temperature was 42℃ and the irradiance was 994 W/m^2, the maximum delta T observed was 42℃. The maximum module temperature observed during this testing period was 94℃, when the irradiance was 994 W/m^2 and ambient temperature was 42℃. This indicates that the modules undergo higher level daily thermal cycling stress during winter as compare to summer.

In order to predict the temperature of thermally insulated BAPV modules, the three-parameter model was used again. A plot correlating the predicted temperature with the actual temperature is shown in Figure 4.7. Table 4.5 shows the thermal model coefficients of the insulated modules. By comparing Table 4.3 (0-in air gap; middle two-column average) with Table 4.5 (all wind speeds) coefficients, the following observations can be made:

- Irradiance coefficient: The back insulation increased the irradiance coefficient by 40% from 0.033 to 0.046.

- Wind speed coefficient: The back insulation dramatically decreased the wind speed coefficient (or increased the WS effect) by 83% from -1.91 to -3.52 (due to large delta T).
- T_{amb} coefficient: The back insulation decreased the T_{amb} coefficient by 34% from 1.08 to 0.71.
- Constant: The back insulation increased the constant value by about 141% from 8.00 to 19.13.

Table 4.4 Highest delta T and highest module temperature between October 2009 and March 2010

	Tmod at highest Delta T	**Highest Tmod**
R30_1 (°C)	78.4	93.7
R30_2 (°C)	75.7	92.3
R30_3 (°C)	75.2	92.1
R30_4 (°C)	75.1	92.2
R30_5 (°C)	74.8	93.1
Average (°C)	75.8	**92.7**
Delta T (°C)	**65.7**	50.8
Irradiance (W/m^2)	1056.6	993.5
T_{amb} (°C)	10.2	41.9
Wind Speed (m/s)	1.5	1.2
Date	02/23/2010	10/17/2009
Time	12:24	12:42

Table 4.5 Thermal model coefficients for insulated BAPV modules

	Back Insulated Module			
	Irr (w1)	T_{amb} (w2)	WS (w3)	Const
at all WS	0.046	0.71	-3.52	19.13
< 4m/s WS	0.048	0.70	-3.89	19.04
< 2m/s WS	0.050	0.64	-2.04	15.82

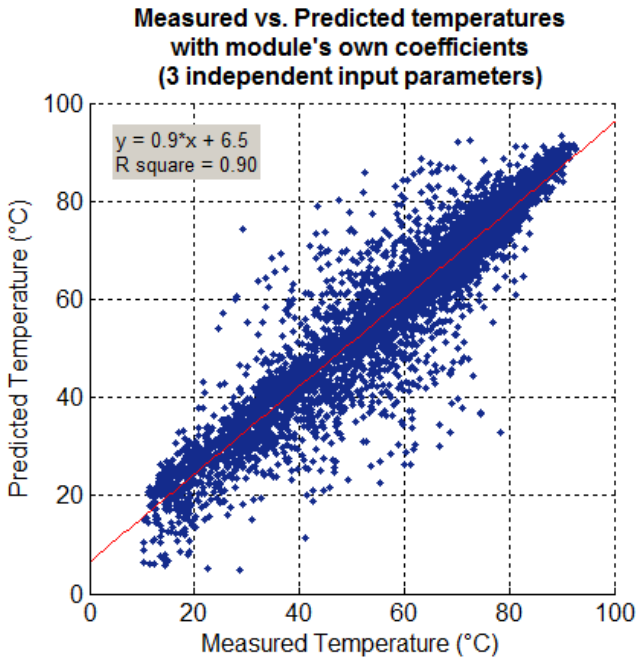

Figure 4.7 Linear correlation between predicted temperature and measured temperature for insulated BAPV modules (October 2009 - March 2010)

4.3 Nominal Operating Cell Temperature of BAPV Modules - Effect of Air Gap

Typically, the measurement of nominal operating cell temperature (NOCT) is done by installing the module on the open rack mount. Thus, the NOCT of the BAPV module, also known as installed NOCT (INOCT), might be different from regular NOCT [9]. The INOCT with effect of air gap is presented in this section.

INOCT obtained for each module based on field data and R^2 values are shown in Table 4.6. The overall R^2 values of column 1 modules are higher than the values of other columns due to the increased effect of wind, which makes the temperature of the module close to ambient temperature. All the INOCT values

shown in Table 4.6 were obtained by using ambient temperature in accordance with the standard procedure. However, BAPV module temperatures are also affected by air-gap temperature, which led to the effort to obtain INOCT using air-gap temperature, as shown in Table 4.7, which shows the results of INOCT using air gap temperature, but the R^2 values were much lower than those found in the measurement of INOCT using ambient temperature. Therefore, INOCT values using averages of ambient temperature and air-gap temperature were also derived in order to get higher R^2 values, as shown in Table 4.8. Table 4.6 and Table 4.8 show that the R^2 values of 3-in and 4-in modules are higher when ambient temperature is used for INOCT, and the R^2 values of 0-in, 1-in, and 2-in modules are higher when the average temperature is used. Also, INOCT of the 4-in air-gap modules was normally lower than INOCT of the 0-in air-gap modules, as shown in Table 4.6.

Table 4.6 NOCT of BAPV modules using ambient temperature

	Column 1 (Poly)		**Column 2 (Mono)**		**Column 3 (Poly)**		**Column 4 (Mono)**	
Air gap (inch)	**INOCT (°C)**	**R^2**	**INOCT (°C)**	**R^2**	**INOCT (°C)**	**R^2**	**INOCT (°C)**	**R^2**
4”	49.0	0.83	49.7	0.89	49.5	0.90	48.9	0.86
3”	51.4	0.89	52.3	0.92	52.0	0.92	53.0	0.80
2”	52.4	0.92	53.8	0.92	53.2	0.85	54.7	0.82
1”	52.6	0.92	49.8	0.80	51.5	0.80	53.6	0.78
0”	53.3	0.91	53.4	0.82	53.8	0.76	55.1	0.80

Table 4.7 NOCT of BAPV modules using air-gap temperature

	Column 1 (Poly)		Column 2 (Mono)		Column 3 (Poly)		Column 4 (Mono)	
Air gap (inch)	**INOCT (°C)**	**R^2**	**INOCT (°C)**	**R^2**	**INOCT (°C)**	**R^2**	**INOCT (°C)**	**R^2**
4”	43.4	0.1851	41.1	0.4211	42.8	0.3886	41.5	0.4284
3”	42.1	0.0025	42.3	0.3535	42.1	0.5070	43.4	0.4592
2”	40.8	0.0409	40.6	0.0883	41.3	0.1704	41.2	0.4387
1”	41.0	0.0352	37.7	0.5702	41.6	0.5308	42.6	0.4552
0”	41.9	0.0164	39.0	0.1422	40.7	0.0601	40.7	0.1026

Table 4.8 NOCT of BAPV modules using the average of ambient and air-gap temperatures.

	Column 1 (Poly)		Column 2 (Mono)		Column 3 (Poly)		Column 4 (Mono)	
Air gap (inch)	**INOCT (°C)**	**R^2**	**INOCT (°C)**	**R^2**	**INOCT (°C)**	**R^2**	**INOCT (°C)**	**R^2**
4”	45.7	0.70	44.9	0.76	45.6	0.78	44.7	0.77
3”	46.7	0.59	47.3	0.82	47.5	0.88	48.7	0.76
2”	46.6	0.66	47.2	0.70	47.3	0.95	48.0	0.92
1”	46.8	0.60	43.8	0.91	46.6	0.88	48.1	0.96
0”	47.6	0.49	45.7	0.88	46.7	0.92	47.4	0.91

Evaluation of INOCT results is shown in Figure 4.8. A column 3 module with a 3-in air gap was selected as a sample for this evaluation. A total of five actual module temperatures that have very close to NOCT condition, such as an irradiance of 800 W/m^2, an ambient temperature of 20°C , a wind speed of 1 m/s, were obtained from one-year actual data. As shown in Table 4.9, INOCT based on T_{amb} is closer to the actual temperature that has the NOCT condition than the INOCT based on $T_{average}$. This is true despite a lower R^2 value for INOCT based on $T_{average}$.

The predicted module temperature that has the NOCT condition using the annual coefficient-based thermal model that is presented in section 4.3 and Appendix A are shown in Figure 4.8. The predicted temperature using the one-year-based thermal model shows a more accurate temperature than using the seasonal-based thermal model, as shown in Table 4.9, and they are all within 2℃ of the actual temperature, as shown in Figure 4.8.

As shown in Figure 4.8, it was observed that INOCT that included the actual measured temperature was about 2℃ higher than NOCT (49.7℃) that was measured by ASU-PTL in 2007. This is the exactly the same result as predicted by the Sandia National Laboratory. According to Sandia's report, INOCT of a roof-mounted PV module with 3-in air-gap spacing is about 2℃ higher than NOCT [9].

Evaluation of INOCT using various methods is shown in Figure 4.9. The first bar is the average of the actual module temperature having around NOCT ambient conditions, and the second bar reflects INOCT from the thermal model that was developed in this study. The last bar is the INOCT using the IEC method. As shown in Figure 4.9, all three temperatures from different methods show similar temperature with less than 1℃ difference.

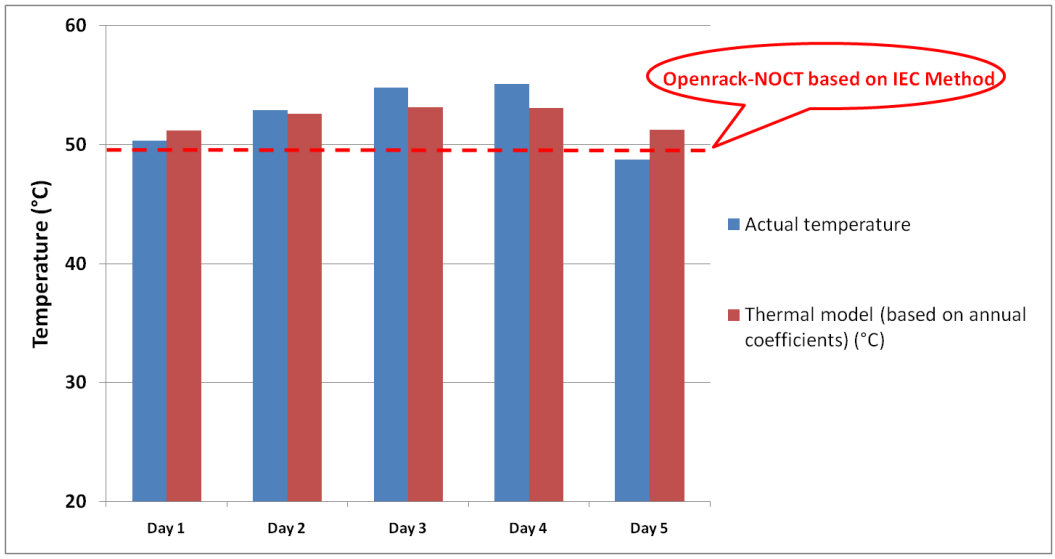

Figure 4.8 NOCT from various methods

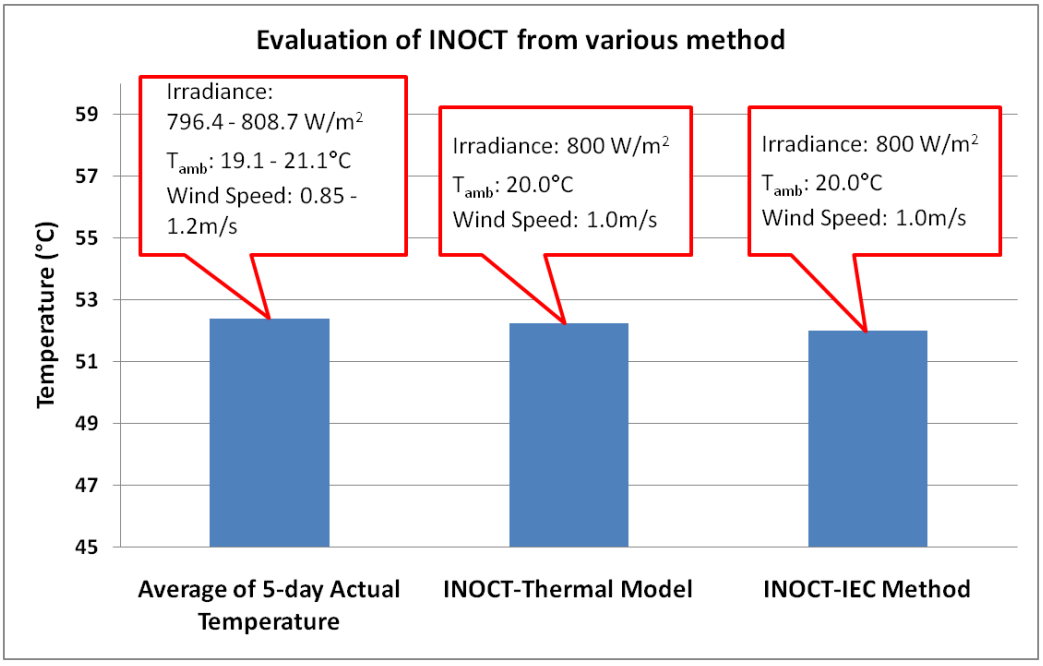

Figure 4.9 INOCT from various methods

Table 4.9 Actual module temperature that has NOCT ambient condition (3-in air-gap module at Column 3)

	Day 1	Day 2	Day 3	Day 4	Day 5	Average
Date	01/08/2010	01/13/2010	01/05/2010	11/18/2009	11/25/2009	
Time	3:00 PM	2:18 PM	2:12 PM	11:36 AM	10:24 AM	
Irradiance	803.8	790.5	808.7	800.7	796.4	800.0
T_{amb}	19.1	21.1	21.1	20.4	19.5	20.3
Wind Speed	1.11	1.18	1.20	0.85	1.15	1.10
Actual temperature (°C)	**50.4**	**52.9**	**54.8**	**55.1**	**48.8**	52.4
Thermal model (based on annual coefficients) (°C)	51.2	52.6	53.1	53.1	51.2	52.2
Thermal model (based on seasonal coefficients) (°C)	53.0	54.8	55.4	52.6	50.7	53.3
INOCT based on T_{amb} (°C)	-	-	52.0	-	-	-
INOCT based on T_{airgap}(°C)	-	-	42.1	-	-	-
INOCT based on $T_{average}$ (°C)	-	-	47.5	-	-	-
INOCT-Thermal Model (°C)	52.3					
Openrack-NOCT based on IEC method (°C)	49.7					

4.4 Nominal Operating Cell Temperature of Back-Insulated BAPV Modules

Three days were chosen for use in determining the NOCT of back-insulated BAPV modules. These modules do not have air-gap spacing, so only the ambient temperature was used for data processing of NOCT. The results are shown in Table 4.10. The average three-day temperature was 67.9℃, which is about 18℃ higher than open-rack NOCT, as shown in Figure 4.9. This temperature is 2 - 3℃ lower than the results that Sandia National Laboratory reported, which was a difference of 20℃. The actual temperature of the back-insulated BAPV module at around NOCT ambient condition is shown in Figure 4.10 and Table 4.11. An average of the actual temperatures for all five days was 66.5℃, which is about 1 - 2℃ different from the three-day average of insulated INOCT. Also, the predicted temperature that was obtained by the R30 thermal model presented in section 4.2 is shown in Table 4.11. It is observed that the five-day temperature average of the actual module was 66.5℃, the average of the insulated INOCT was 67.9℃, and the INOCT based on the R30 thermal model was 66.6℃, which are all close to each other.

Table 4.10 Back-insulated INOCT

Day	**Insulated INOCT (°C)**
Day 1	67.6
Day 2	67.8
Day 3	68.3
3-day average	**67.9**

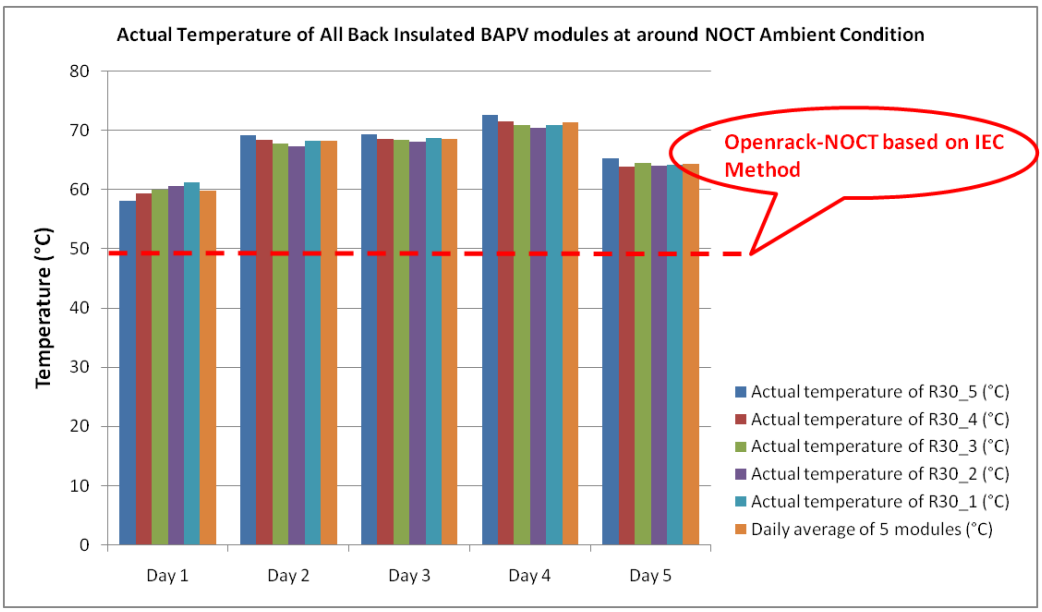

Figure 4.10 Actual temperature of all five back insulated BAPV module at NOCT ambient condition

Table 4.11 Actual temperature of the insulated BAPV modules that has NOCT ambient condition

	Day 1	Day 2	Day 3	Day 4	Day 5	5 day Average
Date	01/08/2010	01/13/2010	01/05/2010	11/18/2009	11/25/2009	
Time	3:00 PM	2:18 PM	2:12 PM	11:36 AM	10:24 AM	
Irradiance (W/m^2)	803.8	790.5	808.7	800.7	796.4	800.0
T_{amb} (°C)	19.1	21.1	21.1	20.4	19.5	20.3
Wind Speed (m/s)	1.11	1.18	1.20	0.85	1.15	1.10
Actual temperature of R30_5 (°C)	58.1	69.2	69.4	72.7	65.3	66.9
Actual temperature of R30_4 (°C)	59.3	68.3	68.5	71.6	63.9	66.3
Actual temperature of R30_3 (°C)	60.0	67.8	68.5	70.9	64.5	66.3
Actual temperature of R30_2 (°C)	60.5	67.3	68.1	70.5	64.1	66.1
Actual temperature of R30_1 (°C)	61.2	68.2	68.7	70.9	64.2	66.6
Daily average of 5 modules (°C)	**59.8**	**68.2**	**68.6**	**71.3**	**64.4**	**66.5**
Thermal model based on R30 coefficients (all WS) (°C)	65.8	66.3	67.1	67.5	65.6	66.5
Thermal model based on R30 coefficients (<2m/s) (°C)	66.0	66.4	67.3	67.2	65.8	66.6
Insulated INOCT-IEC Method (°C)	-	-	67.6	-	-	-
Insulated INOCT-Thermal Model (°C)	66.6					-

4.5 Temperature Testing per IEC 61730 and UL 1703 Method

4.5.1 Open Circuit Condition

The temperatures obtained for each of the components under open-circuit conditions are presented in Figure 4.11. Three types of component temperatures are reported in this figure, i.e., average normalized temperature, maximum normalized temperature, and maximum raw temperature. The average normalized temperature refers to the average of normalized temperatures of 140 modules as per Equation 3.1. The maximum normalized temperature refers to the highest normalized temperature observed out of 140 modules. The maximum raw temperature refers to the highest measured (without normalization) temperature out of 140 modules at the desert climatic site of Mesa/Tempe, Arizona.

The cell, substrate, and front glass experience higher maximum normalized temperatures (92 - 98℃) as compared to all other components (86 - 89℃). The polymeric components (substrate, J-box surface, J-box backsheet, and cables/field wiring) experience the maximum normalized temperatures in the range of 86 - 97℃. Similarly, the diodes experience the maximum normalized temperatures in the range of 88 - 89℃. The normalized maximum cell temperatures of all the 140 modules under open-circuit conditions are presented in the scatter plot of Figure 4.12. The normalized maximum cell temperatures fall between 77 and 98℃, with an average temperature of 87℃.

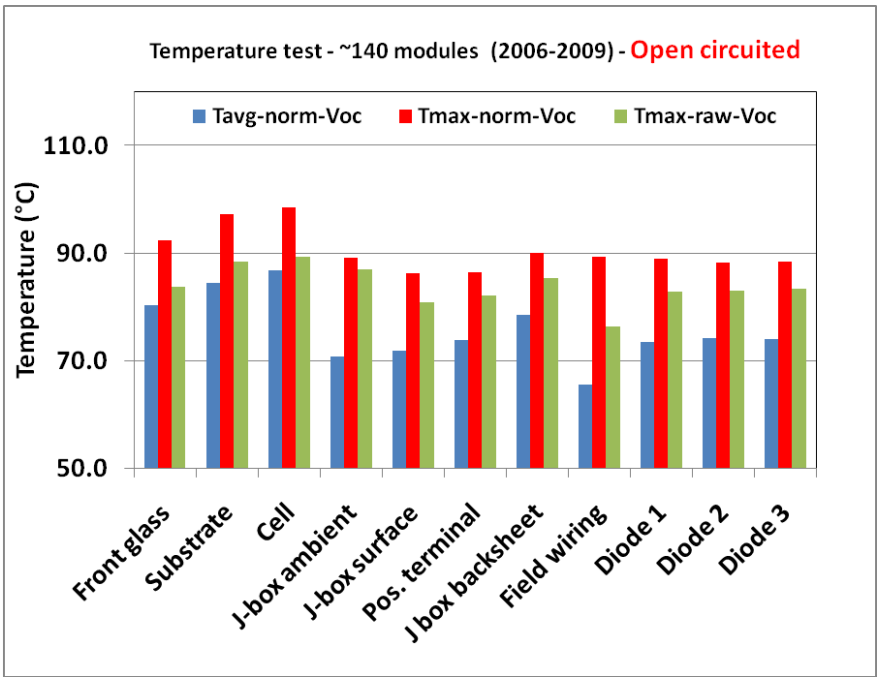

Figure 4.11 Temperature comparisons (open circuit)

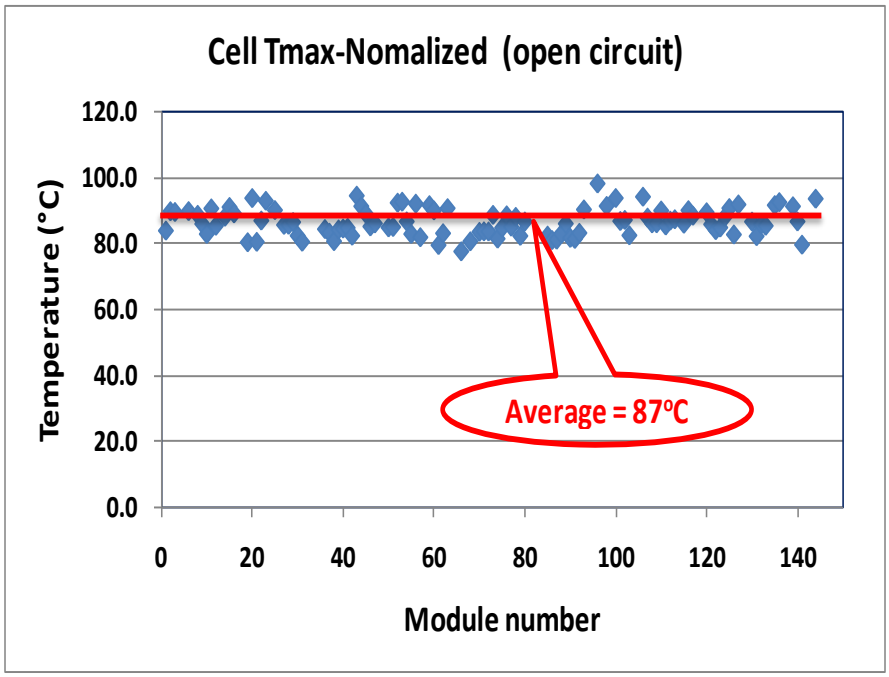

Figure 4.12 Normalized maximum cell temperature (open circuit)

4.5.2 Short-Circuit Condition

As shown in Figure 4.13, the diodes, J-box backsheet and the cell experience higher maximum normalized temperatures (110 - 118℃) as compared to the other components (84 - 107℃) under short-circuit conditions. The polymeric components (substrate, J-box surface, J-box backsheet, and cables/field wiring) experience the maximum normalized temperatures in the range of 85 - 110℃. Similarly, the diodes experience the maximum normalized temperatures in the range of 95 - 118℃.

The normalized maximum cell temperatures of all the 140 modules under short-circuit conditions are presented in the scatter plot of Figure 4.14. The normalized maximum cell temperatures under short-circuit conditions are more scattered as compared to the open-circuit conditions, and they fall mostly between 76 and 109℃. The normalized average cell temperature of 89℃ under short-circuit conditions is about 2℃ higher than at open-circuit conditions. This slightly higher temperature of 2℃ is attributed to I^2R heating of solar cells under short-circuit conditions.

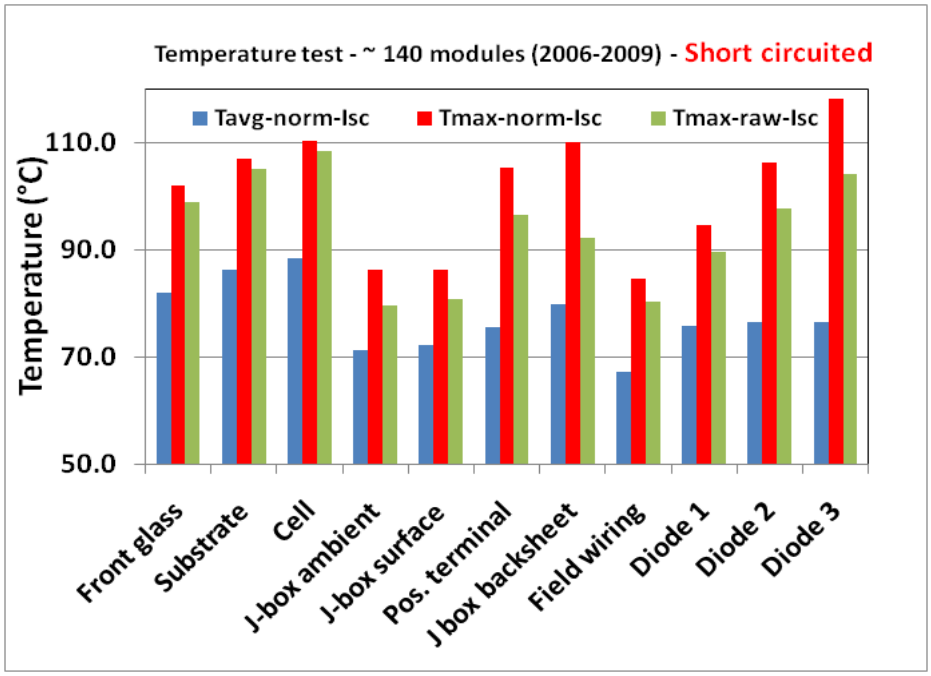

Figure 4.13 Temperature comparisons (short circuit)

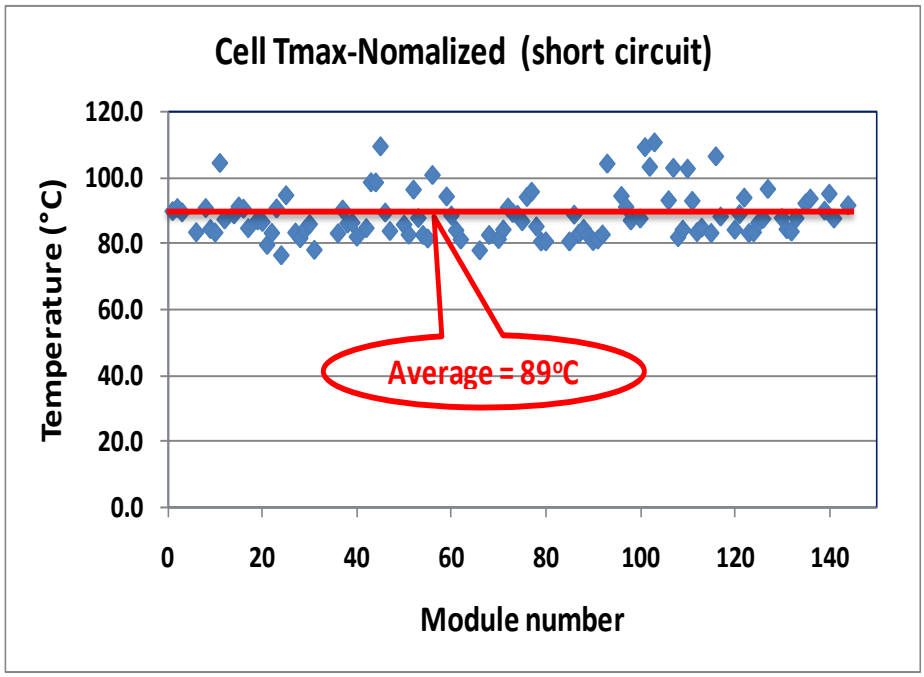

Figure 4.14 Normalized maximum cell temperature (short circuit)

4.5.3 Short and Shaded Condition

The testing under shorted-shaded conditions is required only for the ANSI/UL 1703 procedure, and the results obtained at these conditions are provided in Figures 4.15 and 4.16. As shown in Figure 4.15, the cell, front glass, and substrate experience higher maximum normalized temperatures (158 - 176℃) as compared to the other components (88 - 140℃) under shorted-shaded conditions.

The polymeric components (substrate, J-box surface, J-box backsheet, and cables/field wiring) experience the maximum normalized temperatures in the range of 89 - 158℃. As expected, the diodes experience higher temperatures under shorted-shaded conditions as compared to the other two conditions. The maximum normalized temperatures of the diodes fall in the range of 118 - 140℃.

The normalized maximum cell temperatures of all 140 modules under shorted-shaded conditions are presented in the scatter plot of Figure 4.16. The normalized maximum cell temperatures under shorted-shaded conditions are much more scattered as compared to the open-circuit and short-circuit conditions, and they fall between 80 and 180℃. The normalized average cell temperature of 111℃ under shorted-shaded conditions is about 22℃ higher than that of short-circuit conditions. This huge difference of 22℃ is attributed to the shading effect of solar cells under short-circuit conditions.

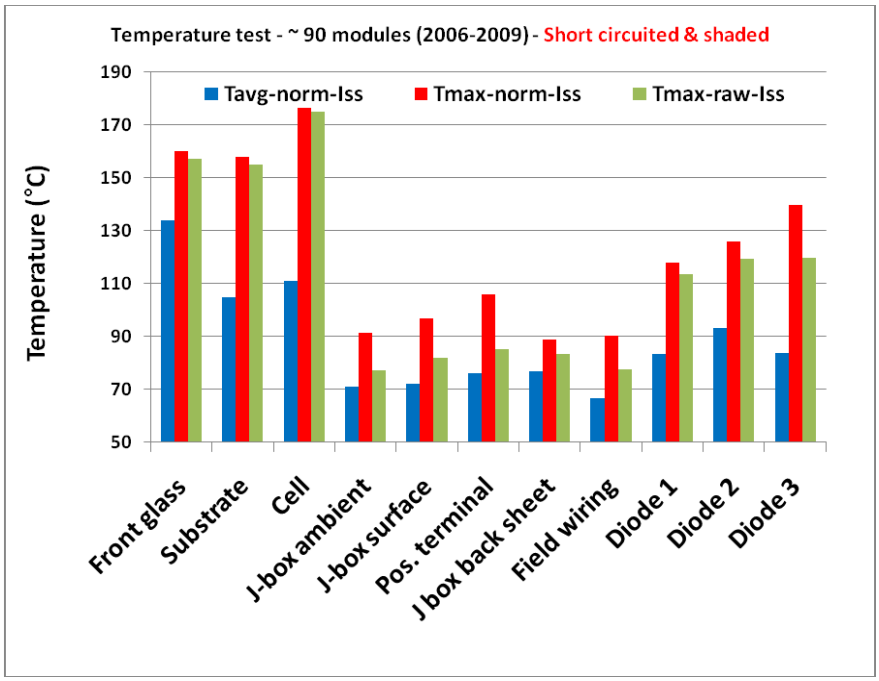

Figure 4.15 Temperature comparisons (shorted-shaded)

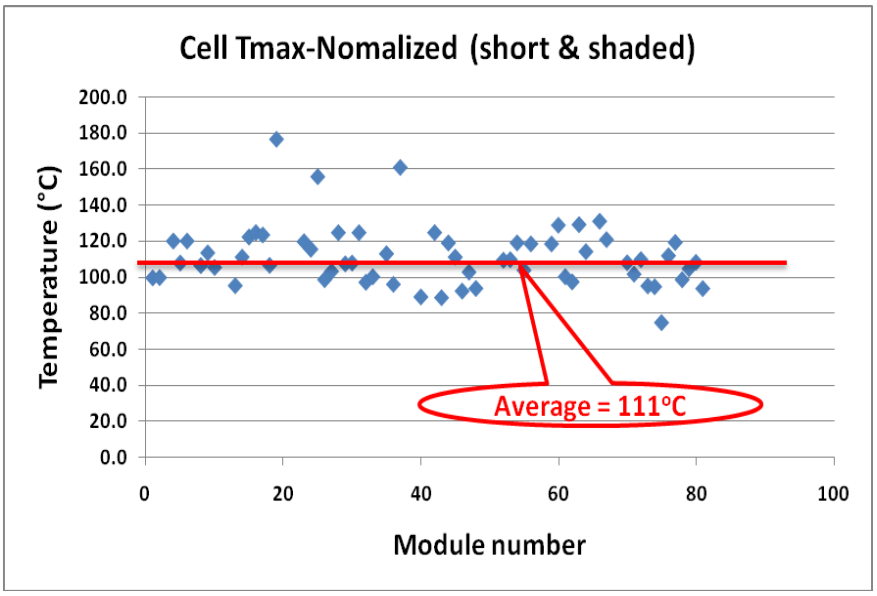

Figure 4.16 Normalized maximum cell temperature (shorted-shaded)

Figure 4.17 presents the average normalized temperatures of all the components under all the bias/electrical termination conditions. These temperatures were found to be lower than 90°C for all the components under

open-circuit and short-circuit conditions. These temperatures could reach as high as 110℃ (excluding the front glass) under shorted-shaded conditions.

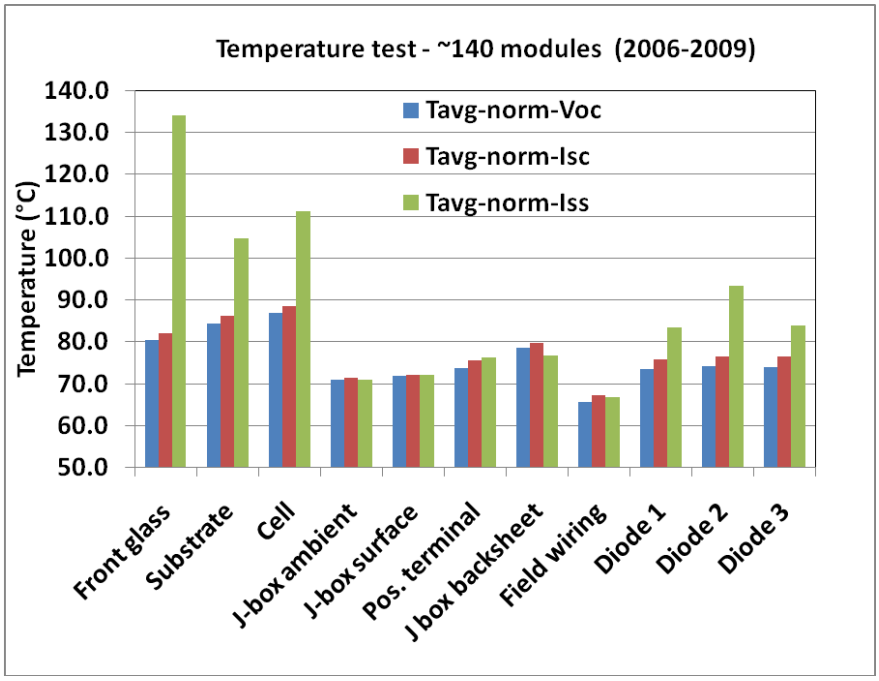

Figure 4.17 Average temperature at each bias condition

CHAPTER 5

CONCLUSIONS AND RECOMMENDATIONS

5.1 Conclusions

5.1.1 Thermal Modeling of BAPV modules – Effect of Air Gap

Thermal models were developed that can be used to predict the temperatures of BAPV modules under various installation conditions (air gaps and columns of modules) and monthly, seasonal, and annual climatic conditions of Arizona. The effect of wind direction on the module temperature is addressed. Since the coefficients of the parameters were determined to be sensitive to seasonal (or even monthly) weather conditions, the coefficients reported in this work may not be applicable to other sites that may not experience weather conditions similar to the current test location (Mesa, Arizona - a hot, dry desert climatic location).

5.1.2 INOCT of BAPV modules – Effect of Air Gap

The INOCT based on ambient temperature is closer to the actual measured module temperature than INOCT based on air-gap temperature or the average of the ambient and air-gap temperatures, irrespective of the R^2 value. The INOCT at 3-in air gap is about 2℃ higher than open-racked NOCT, and insulated INOCT is about 20℃ higher than open-racked NOCT, which means the air-gap effect obviously exists. Therefore, it is suggested that INOCT be used instead of NOCT when the PV module is installed on a roof surface.

5.1.3 Temperature Testing

Based on the temperature test results on 140 glass/polymer modules at the normalized reporting conditions of 40℃ ambient temperature and 1000 W/m^2 irradiance, it is concluded that the:

- Average (T_{avg}) cell temperatures under open, short and short-shaded bias conditions are about 87℃, 89℃ and 111℃, respectively.
- Average (T_{avg}) backsheet temperatures under the V_{oc} and I_{sc} bias conditions are about 2℃ lower than the average cell temperatures (about 6℃ lower for I_{sc}-shaded condition).
- Average (T_{avg}) J-box surface and field wiring temperatures are about 72℃ and 67℃, respectively, irrespective of bias conditions.
- Highest maximum (highest T_{max}) cell, backsheet, J-box surface, and field wiring temperatures were 176℃, 155℃, 97℃ and 90℃, respectively.

Based on these results, it may be prudent to suggest that the PV module polymeric materials may be subjected to:

- long-term thermal stress tests at the "T_{avg}" reference temperature of about 85℃ (backsheet), 72℃ (J-box surface) and 67℃ (field wiring) for durability and reliability issues.
- short-term thermal stress tests at the "highest T_{max}" reference temperature of about 155℃ (backsheet), 97℃ (J-box surface) and 90℃ (field wiring) for fire safety issues.

5.2 Recommendations

The following recommendations are made for future investigation of BAPV thermal modeling, NOCT measurement, and temperature testing:

- The BAPV array in this work consisted of four different module types from four different manufacturers depending on column. It is suggested that one type of module from the same manufacturer be used in order to get more accurate results of air-gap and wind effects;
- In this study, a yearly-, seasonal-, and monthly-based BAPV thermal model was developed for predicting BAPV module temperatures. It is suggested that a daily-based or even a six-minute-based thermal model be developed to get more accurate predictions of the temperatures of the modules;
- The weather data used in BAPV thermal modeling was obtained from the weather station nearby the mock roof. It is recommended that the weather station be installed directly on the mock roof installation;
- The data points obtained for measurement of INOCT were collected every six minutes due to the weather station pre-setup. It is suggested that the data be collected with an interval of less than five seconds, as is required by the IEC standards;
- For temperature testing in this study, only flat-plate crystalline-silicon PV modules were considered for the analysis. It may be necessary to extend the scope to include testing for thin-film PV modules.

REFERENCES

1. Del Cueto JA, *"Comparison of energy production and performance from flat-plate photovoltaic module technologies deployed at fixed tilt,"* Proceeding of the 29th IEEE Photovoltaic specialists conference, New Orleans, LA (2002).

2. King, D.L., Kratochvil, J.A., Boyson, W.E., *"Temperature coefficients for PV modules and arrays: Measurement methods, difficulties, and results,"* Proceeding of the 26th IEEE Photovoltaic Specialists Conference, Anaheim, CA (1997).

3. Whitaker, C and Newmiller, J, *Photovoltaic Module Energy Rating Procedure*, Final subcontract report, NREL/SR-520-23942, National Renewable Energy Laboratory, CO (1998)

4. Green, M. Solar Cells, *Operating principles, Technology and System Applications,* Prentice hall, Inc., Eaglewood Cliffs, N.J, page 114 (1982)

5. Design qualification Type approval of commercial PV Modules, *IEC 61215 10.6 Performance at NOCT with IEC 60904-3 reference solar spectral irradiance distribution* (2005)

6. Yingtang Tang's: *Outdoor Energy Rating Measurements of Photovoltaic Modules*, Masters' Degree Thesis Report, Arizona State University (2005)

7. IEC 61853. *Draft Performance Testing and Energy Rating of Terrestrial Photovoltaic*

8. Shrestha, B. L., Palomino, E.G., and TamizhMani, G., *Temperature of rooftop photovoltaic modules: air gap effects*, Proceeding of the SPIE Conference, San Diego, CA (2009)

9. Fuentes, M.K., *A Simplified Thermal Model for Flat-Plate Photovoltaic Arrays*, SAND85-0330.UC-63, Sandia National Laboratories, NM (1987)

10. Oh, J and Tamizhmani, G., *Temperature Testing and Analysis of PV Modules per ANSI/UL 1703 and IEC 61730 Standards*, Proceeding of the 35th IEEE Photovoltaic Specialists Conference, Honolulu, HI (2010)

11. Oh, J., Tamizhmani, G., Palomino, E.G., *Temperatures of Building Applied Photovoltaic (BAPV) Modules: Air Gap Effects*, Proceeding of the SPIE Conference, San Diego, CA (2010)

12. International Electrotechnical Commission (IEC) standard, IEC 61215 (2005)

13. International Electrotechnical Commission (IEC) standard, IEC 61730-2 (2004).

14. American National Standards Institute (ANSI) and Underwriters Laboratories (UL) standard, ANSI/UL 1703 (2004)

15. Bijay L. Shrestha's Thesis: *Temperature of Rooftop PV Modules: Effect of Air Gap and Ambient Condition*, Master's Degree Thesis Report, Arizona State University (2009)

APPENDIX A

SEASONAL AND ANNUAL THERMAL MODEL COEFFICIENTS

(DATA COLLECTED MAY 2009 – APRIL 2010)

		Mnf 1/Column 1(Poly)				Mnf 2/Column 2(Mono)				Mnf 3/Column 3(Poly)				Mnf 4/Column 4(Mono)			
		Irr (w1)	T_{amb} (w2)	WS (w3)	Const	Irr (w1)	T_{amb} (w2)	WS (w3)	Const	Irr (w1)	T_{amb} (w2)	WS (w3)	Const	Irr (w1)	T_{amb} (w2)	WS (w3)	Const
4inch air-gap	Spring	0.023	0.81	-2.01	11.16	0.023	0.97	-2.27	5.67	0.025	1.15	-2.60	6.75	0.023	1.27	-2.85	4.24
	Summer	0.032	0.53	-2.45	17.57	0.031	0.76	-3.03	10.46	0.030	1.03	-3.18	9.47	0.027	1.18	-3.21	4.95
	Fall	0.028	0.74	-2.98	14.27	0.029	0.73	-3.11	14.55	0.028	1.05	-3.20	10.12	0.026	1.06	-3.12	10.30
	Winter	0.031	0.89	-3.16	10.98	0.032	0.90	-2.92	10.40	0.031	1.23	-2.92	5.93	0.028	1.24	-2.93	6.38
	Average	0.028	0.74	-2.65	13.49	0.029	0.84	-2.83	10.27	0.028	1.12	-2.97	8.07	0.026	1.19	-3.03	6.47
	1 year	0.029	0.66	-2.99	14.93	0.030	0.64	-3.08	15.35	0.029	1.02	-3.12	9.95	0.027	1.06	-3.07	9.67
3inch air-gap	Spring	0.026	1.00	-2.08	5.49	0.025	1.04	-2.32	4.98	0.027	1.16	-2.57	7.56	0.025	1.33	-2.75	5.19
	Summer	0.034	0.68	-2.64	13.56	0.032	0.81	-2.68	10.05	0.032	1.07	-2.83	7.92	0.030	1.26	-3.14	5.42
	Fall	0.031	0.78	-2.86	13.75	0.031	0.76	-2.85	14.65	0.029	1.04	-2.87	10.62	0.029	1.11	-2.84	11.06
	Winter	0.034	0.92	-2.83	10.05	0.033	0.98	-2.42	9.78	0.034	1.23	-2.62	5.08	0.031	1.36	-2.61	5.84
	Average	0.031	0.85	-2.60	10.71	0.030	0.90	-2.57	9.87	0.030	1.13	-2.72	7.79	0.029	1.27	-2.84	6.87
	1 year	0.032	0.69	-2.85	14.45	0.032	0.67	-2.75	15.66	0.031	1.02	-2.85	9.90	0.030	1.10	-2.89	10.77
2inch air-gap	Spring	0.027	1.14	-1.60	-0.28	0.027	1.02	-1.66	4.53	0.028	1.21	-2.04	6.11	0.028	1.27	-2.25	6.73
	Summer	0.035	0.76	-2.33	9.64	0.034	0.85	-1.97	7.77	0.035	1.08	-2.09	6.16	0.033	1.25	-2.35	4.77
	Fall	0.031	0.80	-2.47	13.05	0.032	0.79	-2.17	13.53	0.030	1.09	-2.02	9.37	0.031	1.15	-2.33	9.94
	Winter	0.035	0.99	-2.41	8.03	0.036	1.00	-2.22	8.56	0.035	1.33	-2.13	3.56	0.034	1.36	-2.17	5.56
	Average	0.032	0.92	-2.20	7.61	0.032	0.91	-2.00	8.60	0.032	1.18	-2.07	6.30	0.031	1.26	-2.28	6.75
	1 year	0.033	0.72	-2.53	13.09	0.034	0.70	-2.27	14.02	0.033	1.05	-2.20	8.80	0.032	1.12	-2.34	10.05
1inch air-gap	Spring	0.028	1.01	-1.32	4.81	0.027	1.18	-1.43	5.77	0.029	1.18	-1.63	6.39	0.029	1.34	-1.86	3.43
	Summer	0.033	0.88	-2.20	7.11	0.030	1.25	-2.16	0.59	0.031	1.21	-2.03	3.74	0.033	1.09	-1.82	7.46
	Fall	0.031	0.81	-2.35	12.73	0.028	1.09	-1.91	8.04	0.030	1.11	-1.88	7.72	0.028	1.15	-1.90	10.47
	Winter	0.034	1.00	-2.44	8.74	0.031	1.34	-1.64	2.90	0.033	1.29	-1.93	3.99	0.033	1.37	-2.04	4.96
	Average	0.032	0.92	-2.08	8.35	0.029	1.21	-1.78	4.32	0.031	1.19	-1.87	5.46	0.031	1.24	-1.91	6.58
	1 year	0.033	0.74	-2.31	12.78	0.030	1.09	-1.78	7.00	0.032	1.10	-1.91	7.16	0.032	1.10	-2.02	9.35
0inch air-gap	Spring	0.030	0.93	-1.32	7.09	0.031	1.24	-1.42	4.09	0.031	1.24	-1.54	5.08	0.031	1.48	-2.36	0.54
	Summer	0.032	0.92	-1.73	6.21	0.032	1.22	-2.27	3.68	0.032	1.27	-2.22	2.17	0.032	1.43	-2.55	-0.15
	Fall	0.032	0.79	-2.08	12.44	0.031	1.06	-1.94	9.15	0.031	1.06	-1.92	9.30	0.031	1.13	-2.10	10.31
	Winter	0.035	0.96	-2.16	8.73	0.035	1.34	-1.91	3.19	0.035	1.34	-1.83	3.65	0.034	1.43	-2.00	4.32
	Average	0.032	0.90	-1.82	8.62	0.032	1.21	-1.89	5.03	0.032	1.23	-1.88	5.05	0.032	1.37	-2.25	3.76
	1 year	0.034	0.74	-2.02	12.44	0.033	1.08	-1.94	7.92	0.033	1.08	-1.89	8.09	0.033	1.17	-2.16	8.69

Spring: Mar 21 – Jun 20
Summer: Jun 21 – Sep 20
Fall: Sep 21 – Dec 20
Winter: Dec 21 – Mar 20
Average: Average of all seasons' coefficients
1 year: Coefficients from the entire year data processing

APPENDIX B

MONTHLY THERMAL MODEL COEFFICIENTS OF COLUMN 3 MODULES (DATA COLLECTED MAY 2009 – APRIL 2010)

Month	Air Gap (inch)	Irr (w_1)	T_{amb} (w_2)	WS (w_3)	Constant
Jan	4	0.033	1.11	-3.12	6.28
	3	0.035	1.13	-2.68	5.87
	2	0.036	1.26	-1.69	3.30
	1	0.033	1.23	-1.53	3.91
	0	0.035	1.28	-1.60	3.65
Feb	4	0.032	1.25	-3.43	5.73
	3	0.034	1.29	-3.19	5.38
	2	0.035	1.36	-2.49	3.48
	1	0.034	1.31	-2.29	3.81
	0	0.035	1.37	-2.27	3.59
Mar	4	0.023	1.69	-2.47	5.56
	3	0.026	1.64	-2.49	6.42
	2	0.029	1.63	-2.22	6.55
	1	0.028	1.59	-2.09	6.59
	0	0.030	1.58	-1.94	6.44
Apr*	4	0.033	0.67	-1.82	11.44
	3	0.034	0.68	-1.66	12.90
	2	0.032	0.87	-1.18	13.54
	1	0.031	0.86	-1.19	13.40
	0	0.032	0.83	-0.89	14.90
May	4	0.031	0.97	-1.73	6.15
	3	0.033	0.99	-1.58	6.02
	2	0.034	1.05	-1.17	3.99
	1	0.034	1.06	-0.91	3.97
	0	0.036	1.13	-0.85	1.88
Jun	4	0.021	1.12	-2.99	12.17
	3	0.023	1.11	-2.94	13.25
	2	0.025	1.16	-2.47	11.87
	1	0.026	1.14	-2.10	12.01
	0	0.027	1.18	-2.07	11.97

Month	Air Gap (inch)	Irr (w_1)	T_{amb} (w_2)	WS (w_3)	Constant
Jul	4	0.032	0.64	-2.18	22.28
	3	0.034	0.75	-2.08	17.57
	2	0.040	0.64	-1.63	19.75
	1	0.033	0.99	-1.59	10.26
	0	0.034	1.15	-1.97	5.40
Aug	4	0.028	1.13	-3.03	6.11
	3	0.030	1.16	-2.61	4.37
	2	0.031	1.23	-1.65	1.64
	1	0.030	1.32	-1.71	-1.28
	0	0.031	1.39	-1.78	-3.41
Sep	4	0.034	1.09	-3.70	4.94
	3	0.035	1.13	-3.38	3.70
	2	0.035	1.26	-2.67	0.54
	1	0.033	1.27	-2.68	1.02
	0	0.033	1.35	-2.76	-0.92
Oct	4	0.020	1.19	-4.14	14.14
	3	0.022	1.21	-3.81	14.11
	2	0.023	1.26	-2.81	12.79
	1	0.022	1.21	-2.74	13.57
	0	0.022	1.16	-2.93	16.24
Nov	4	0.030	1.01	-2.22	7.01
	3	0.033	1.00	-1.87	7.09
	2	0.034	1.09	-1.25	4.65
	1	0.033	1.12	-1.08	3.54
	0	0.035	1.09	-1.11	4.85
Dec	4	0.031	1.22	-3.07	5.76
	3	0.033	1.19	-2.88	6.33
	2	0.036	1.24	-2.20	4.03
	1	0.033	1.22	-1.96	4.23
	0	0.036	1.29	-1.75	3.53

* The wind speed data of April 2010 was not available due to unexpected technical difficulties at ASU-PRL, Mesa. Therefore, the wind speed data of April 2010 obtained from APS Solar Test and Research (STAR) center, Tempe (22 miles west of ASU-PRL) and from SRP, Pinal county (13 miles east of ASU-PRL) was adjusted for the ASU-PRL site. Since the wind speed has only second order effect, it is deteremined that this adjustment would have little or no influence on the predicted temperature even though the wind speed coefficient may not be perfectly accurate.